JOURNAL OF GEOPHYSICAL RESEARCH, VOL. 108, NO. B1, 2040, doi:10.1029/2001JB001095, 2003

The Central Basin Spreading Center in the Philippine Sea: Structure of an extinct spreading center and implications for marginal basin formation

Kyoko Okino
Ocean Research Institute, University of Tokyo, Tokyo, Japan

Kantaro Fujioka
Japan Marine Science and Technology Center, Yokosuka, Japan

Received 14 August 2001; revised 25 June 2002; accepted 23 August 2002; published 25 January 2003.

[1] Newly acquired marine geophysical data along the Central Basin Spreading Center (CBSC), the extinct spreading axis of the West Philippine Basin (WPB), display along-axis variations of spreading style. We have described and analyzed the tectonic spreading fabric and segmentation patterns along a 1000-km-long section of the fossil ridge between 126°00′ and 133°30′E. ''Slow-spreading features'' (deep rift valleys and nodal basins, rough abyssal hills on the ridge flanks, and mantle Bouguer anomaly lows beneath segment centers) are observed in the eastern CBSC. In contrast, ''fast-spreading'' features (overlapping spreading centers, volcanic axial ridges, and smooth abyssal hill fabric) are identified along the western CBSC. We attribute the large morphological and geophysical variations along the CBSC to higher melt supply in the western region caused by high mantle temperature and/or mantle heterogeneity, which may be related to a relatively small-scale mantle plume forming the oceanic plateaus located in the WPB. Another prominent feature of the CBSC is the development of a deep valley oblique to the spreading fabric. Reconstructions of the plate boundary geometry through time, using abyssal hill geometry as well as other measurements, provide evidence for a later stage of amagmatic extension (i.e., reactivation) along the CBSC after the formation of the main basin. This stage is dominated by tectonic deformation with minor amounts of volcanism (mainly located in eastern segments), resulting in the observed surface brittle deformation distributed within a broad zone of ductile deformation. *INDEX TERMS:* 3035 Marine Geology and Geophysics: Midocean ridge processes; 3045 Marine Geology and Geophysics: Seafloor morphology and bottom photography; 3010 Marine Geology and Geophysics: Gravity; 3040 Marine Geology and Geophysics: Plate tectonics (8150, 8155, 8157, 8158); 3005 Marine Geology and Geophysics: Geomagnetism (1550); *KEYWORDS:* marginal basin formation, seafloor morphology, extinct spreading center, Philippine Sea

Citation: Okino, K., and K. Fujioka, The Central Basin Spreading Center in the Philippine Sea: Structure of an extinct spreading center and implications for marginal basin formation, *J. Geophys. Res.*, *108*(B1), 2040, doi:10.1029/2001JB001095, 2003.

1. Introduction

[2] Geophysical and geochemical observations combined with model studies show that one key parameter controlling mid-ocean ridge processes is the spreading rate [*MacDonald*, 1988; *Parmentier and Phipps-Morgan*, 1990; *Lin and Phipps-Morgan*, 1992]. Recent studies have pointed out that mantle temperatures [e.g., *Cochran et al.*, 1997] and chemical heterogeneities in the upper mantle [*Niu et al.*, 2001] are also critical factors governing ridge process. Ridge morphology, gravity signature, chemical variability, and segment geometry exhibit large variations between fast-spreading and slow-spreading ridges, and the transition occurs at spreading rates in the 50–80 mm/yr. range [*Small*, 1994]. How plate kinematics, mantle upwelling, and decompression melting variations result in such large differences is a basic question in understanding crustal accretion. Most of our knowledge of accretion processes is based on studies of active fast-spreading and slow-spreading midocean ridges, primarily the East Pacific Rise and the northern Mid-Atlantic Ridge. Spreading systems in marginal basins are important sites of crustal accretion; however, back arc basins and other marginal basins have not been studied from the perspective of morphotectonic variations nearly as intensely as have been fast-spreading and slow-spreading midocean ridges. Back arc basins often show more complicated tectonic fabric, higher heat flow values, greater depths, and different basalt chemistry. In this paper we present the morphological and geophysical characteristics along an extinct spreading center in a marginal basin, the Central Basin Spreading Center (CBSC), in the western Philippine Sea. The CBSC is

0148-0227/03/2001JB001095$09.00

considered to have ceased spreading in the middle Oligocene. Satellite gravity data suggest that the spreading system is located near oceanic plateaus and seamount chains in its western part and is connected to the remnant arc at its eastern end. The CBSC provides an ideal setting for the investigation of the influence of anomalous magmatic processes on ridge morphology, and also provides new insight into structural, morphological, and volcanological changes that might occur during the death of a spreading system.

[3] We have conducted a detailed geophysical and petrologic analysis of the CBSC between 126°00′ and 133°30′E with the goal of understanding the tectonics of the Philippine Sea, which is a complex of active and extinct marginal basins and arcs. The CBSC is a long NW-SE-trending structure located in the western Philippine Sea and is considered to be the Eocene-middle Oligocene spreading center of the West Philippine Basin (WPB) [*Hilde and Lee*, 1984]. In spite of their importance for understanding crustal accretion processes in marginal basins in general (and the early history of the Philippine Sea Plate in particular), no systematic, combined morphological and geophysical surveys of back arc spreading centers have been conducted before our cruises. We compiled data acquired during the STEPS (Structure, Tectonics, and Environmental Studies of the Philippine Sea) cruises from 1998 to 2000, which covered the spreading axes, as well as up to 45 km of off-axis coverage. Our bathymetric and gravimetric analyses show large along-axis variations in the style of spreading features of the CBSC. These range from ''fast-spreading'' features such as overlapping spreading centers in the west to ''slow-spreading'' features such as rough abyssal hills, nontransform discontinuities and segment-center mantle Bouguer anomaly (MBA) minima in the east. We propose that these characteristics reflect different thermal histories and/or mantle heterogeneity beneath these distinct regions along the CBSC. The NW-SE-trending deep valley and lineaments that are overprinted on the north-south spreading fabric indicate later extension/deformation after the main stage of basin formation. Our results provide constraints on the crustal accretion processes of the CBSC and their relationship to the evolution of this marginal basin.

2. Overview of the Western Philippine Sea

[4] The western Philippine Sea consists of two distinct regions, the northern Daito Ridge province and the southern WPB (Figure 1). The features of the Daito Ridge province have been interpreted as Paleocene to Eocene remnant arcs [e.g., *Karig*, 1975; *Mizuno et al.*, 1978; *Klein and Kobayashi*, 1981; *Tokuyama et al.*, 1986] and continental fragments [*Nur and Ben-Avraham*, 1982]. The WPB is the oldest basin in the Philippine Sea Plate and has been attributed to back arc spreading [*Karig*, 1975] or to trapping of normal ocean crust in a back arc position [*Uyeda and Ben-Avraham*, 1972; *Hilde and Lee*, 1984]. Previous mapping of seafloor fabrics and identification of magnetic lineations show that it was formed by NE-SW spreading from the CBSC followed by north-south extension from Eocene to Oligocene [*Ben-Avraham et al.*, 1972; *Louden*, 1976; *Hilde and Lee*, 1984]. Drilling results [*Ozima et al.*, 1977; *Kroenke et al.*, 1980] give some constraints for the reconstruction of the WPB; however, no widely accepted models of the early history of the Philippine Sea Plate have emerged [*Seno and Maruyama*, 1984; *Haston and Fuller*, 1991; *Hall et al.*, 1995]. One general consensus is that the CBSC is a remnant spreading center; however, systematic geophysical surveys along the axis had not been completed until our cruises [*Fujioka et al.*, 1999].

2.1. The WPB

[5] The WPB occupies the western part of the Philippine Sea, extending from 5° to 23°N and is the largest and deepest inactive basin on the Philippine Sea Plate. The average depth of the basin ranges from 5500 to 6000 m, deeper than that expected from the standard age-depth curve but in accord with the curve derived for back arc basins [*Sclater*, 1972; *Park et al.*, 1990]. The WPB is bounded on the east side by the Kyushu-Palau Ridge and the Tobi Ridge, on the west side by the Ryukyu (Nansei-Shoto)-Taiwan-Philippine arc-trench system, and on the northern side by the Daito Ridges (Figure 1). Two midplate plateaus, the Benham Rise and the Urdaneta Plateau, are located in the western part of the basin.

[6] Most previous studies concluded that the WPB was spread symmetrically from the CBSC, though interpretation and identification of magnetic anomalies differ. Proposed ages for the cessation of spreading include 39 [*Louden*, 1976; *Mrozowski et al.*, 1982], 26 [*Shih*, 1980], and 35 Ma [*Hilde and Lee*, 1984]. *Shih* [1980] first mapped offsets of the lineation patterns in the basin, and *Lewis and Hayes* [1980] pointed out that several fracture zones offset the CBSC by. *Hilde and Lee* [1984] mapped more than 10 fracture zones in the middle of the basin and concluded that north-south spreading followed earlier NE-SW spreading, in contrast to earlier studies that proposed simple NE-SW spreading.

[7] In the central part of the basin, the orientation of the spreading-generated abyssal hill fabric changes systematically from NW-SE away from the CBSC, to WNW-ESE, to east-west near the CBSC. A southerly facing, WNW-ESE trending, steep escarpment named the Oki Daito Escarpment (ODE) is found in the northern part of the basin [*Ohara et al.*, 1997]. The spreading fabric of the basin floor changes abruptly against this escarpment; the trend is nearly north-south in the north and NW-SE in the south. The east-west/NE-SW curvilinear feature at 8°–10°N revealed by satellite altimetry data [*Sandwell and Smith*, 1997] may be one candidate for an ODE counterpart south of the CBSC [*Okino et al.*, 1999].

[8] Deep sea drilling was carried out in the WPB during Deep Sea Drilling Project (DSDP) Legs 31 and 59 [*Scott and Kroenke*, 1980]. Sites 292 and 293 were located on two plateaus, and Sites 290, 291, 294, 295, and 447 were located on the basin floor (Figure 2). At Site 291, in the southwestern part of the basin, the basement basalt is overlain by late Eocene (37.5–43 Ma) sediments [*Louden*, 1976]. At Sites 294 and 295, in the northern WPB, the age of the basement basalt was determined to be 49 Ma by $^{40}Ar/^{39}Ar$ dating [*Ozima et al.*, 1977]. Sites 290 and 447 are separated by only 35 km in the eastern WPB. At Site 290, the sediment was penetrated up to 255 m, but the basement was not contacted. Volcanic conglomerates and breccia with Eocene-Oligocene (about 37.5 Ma) fossils were recovered; thus *Karig* [1975] suggested that the age of the basal sedimentary unit represented the basement age. At Site 447, the basalt unit was

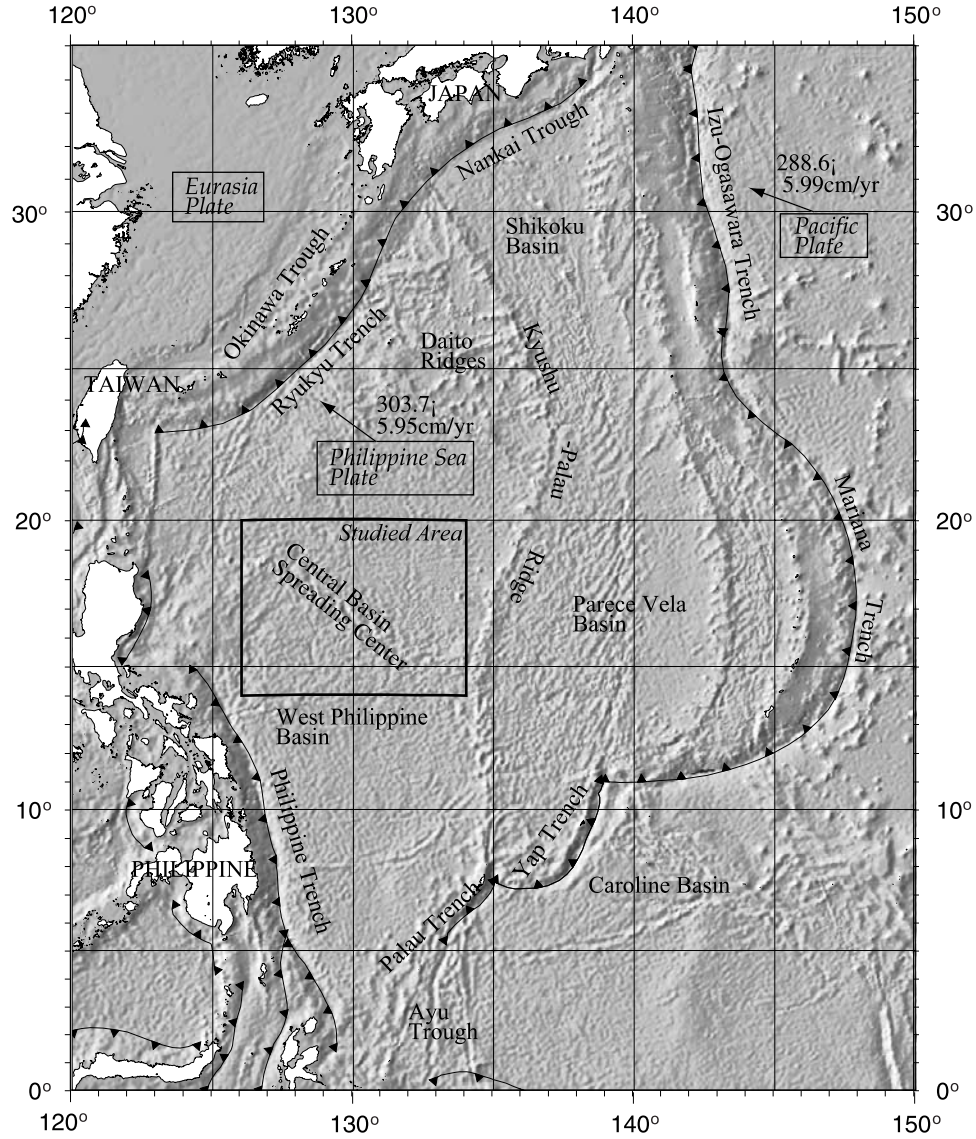

Figure 1. Tectonic setting of the Philippine Sea Plate and surrounding areas overlaid on shaded predicted bathymetry [*Smith and Sandwell*, 1997]. The arrows indicate the current relative plate motions [*DeMets et al.*, 1990]. The box indicates the area illustrated in Figures 3, 4, 5, 6, and 7.

overlain by Middle Oligocene (29–34 Ma) sediment; however, a hiatus may be present at the sediment/basalt contact [*Kroenke et al.*, 1980].

2.2. The CBSC

[9] TheCBSC is a prominent linear bathymetric feature first described by *Hess* [1948] as a NW-SE-trending transcurrent fault. He named it the Central Basin Fault (CBF); therefore some previous studies used the name CBF instead of CBSC.

[10] Until recently, the CBSC has not been systematically mapped and studied, although some ship bathymetry tracks from transits crossed this area. Satellite-derived gravity and bathymetry data [*Sandwell and Smith*, 1997; *Smith and Sandwell*, 1997] reveal that the CBSC consists of east-west-trending segments, providing support for the *Hilde and Lee* [1984] model. During two submersible dives on rift walls of the CBSC at 130°10′E, exposed talus blocks, steep manganese-coated outcrops, and some slightly altered pillow basalts and breccias were observed [*Fujioka et al.*, 1997]. Age dating was carried out on the collected samples, and the ages range between 28.1 and 14.88 Ma [*Fujioka et al.*, 1999]. These ages are considerably younger than those expected from previous models based on magnetic anomalies and drilling results. In 1996 the French ship R/V *l'Atalante* acquired a single-swath NW-SE transect along the CBSC [*Deschamps et al.*, 1999]. Several rhomboidal structures in the vicinity of the rift valley were found and were attributed to dextral shear along the rift axis during the last spreading phase. *Deschamps et al.* [1999] also proposed that the east-west spreading fabrics were crosscut during a final, largely amagmatic, extensional phase to produce a 130°-trending deep rift valley. *Fujioka et al.* [1999] compiled the survey results of R/V *Kairei* in 1998 and showed that the morphological characteristics of the CBSC around 128°30′E were similar to a typical slow spreading center. Interpretation of these previous data and of bathymetry and geophysical data presented below eluci-

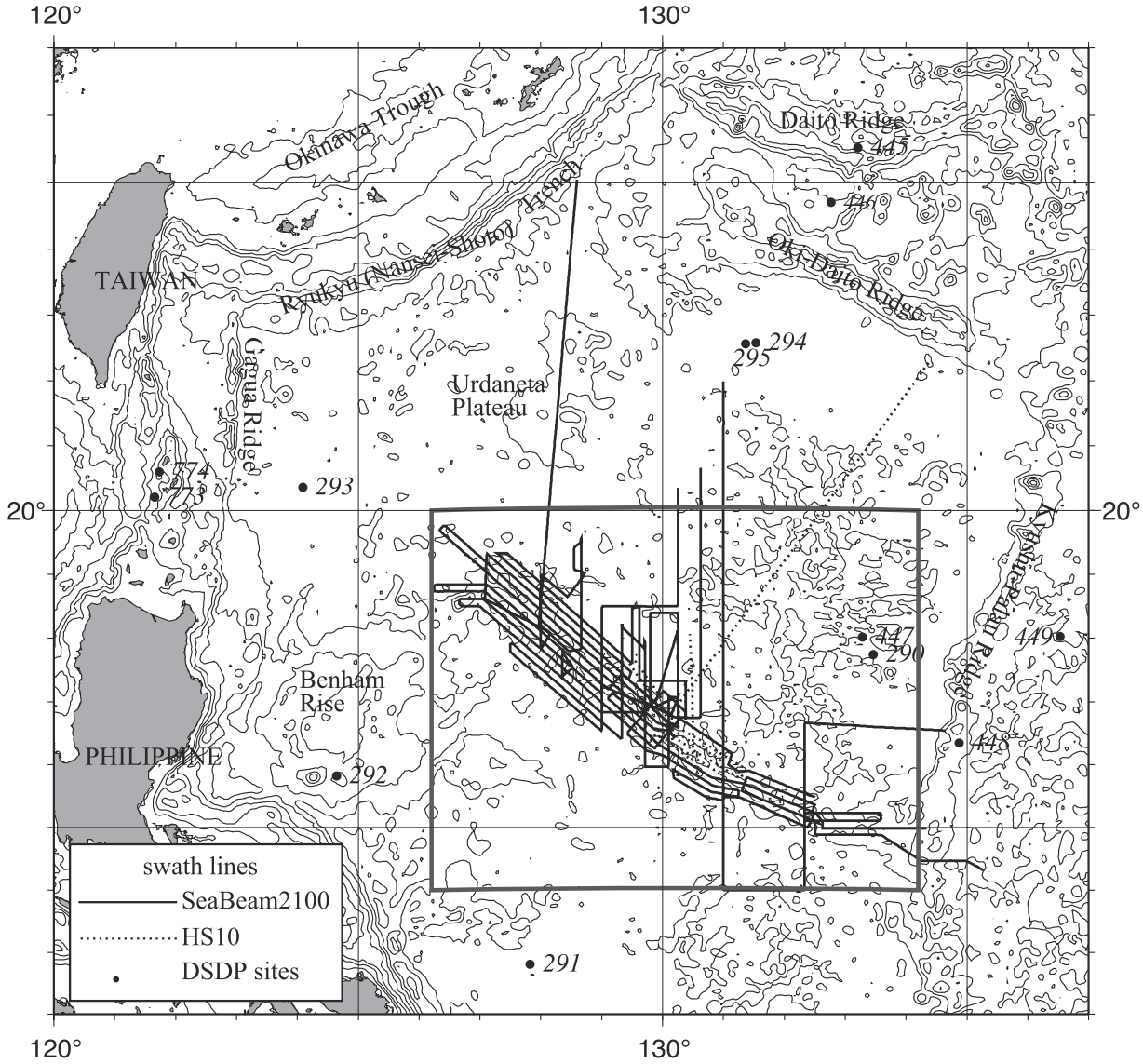

Figure 2. Track chart of the study area. Ship tracks from SeaBeam 2100 and HS 10 cruises are indicated by solid bold and dotted lines, respectively. Closed circles are the previous drilling sites in the DSDP.

date a more complex pattern and large along-axis variations of the rift structure.

3. Data

[11] Between 1998 and 2000, R/V *Kairei* and R/V *Yokosuka* conducted geological and geophysical surveys of the CBSC. During these cruises (KR9801, KR9812, KR9910, and YK0001), swath bathymetry, using SeaBeam 2100, underway gravity, and magnetic data were collected as well as dredge and piston core samples [*Fujioka et al.*, 1998, 1999, 2000; *Yamazaki et al.*, 1999]. The primary track lines were set NW-SE along the general trend of the CBSC at a spacing of 7 nautical miles, resulting in almost complete coverage within 45 km of the axis, except for some local topographic highs (Figure 2). The survey area spans from 131°00′E, the junction of the CBSC and the remnant island arc of the Kyushu-Palau Ridge, to 126°30′E, where the prominent rift valley of the CBSC cannot be followed on the satellite-derived gravity anomaly map [*Sandwell and Smith*, 1997]. Additional swath bathymetry data from the R/V *Yokosuka* have been merged, although these data were collected using the lower-resolution HS-10 system. We utilized Generic Mapping Tools (GMT) [*Wessel and Smith*, 1998] and the MB system [*Caress and Chayes*, 1996] for filtering, gridding, and plotting data sets.

[12] The SeaBeam 2112 is a multibeam survey system that generates data for and produces wide-swath contour maps and side-scan images. The system consists of a 12-kHz projector array along the ship's keel and a hydrophone array across the projector. SeaBeam 2112 synthesizes 2° by 2° narrow beams at an interval of 1°, and the swath width varies from 120° at intermediate depth to 90° in deeper water. The ping interval increases with water depth, for example about 13 s at 4000 m. The accuracy of the depth measurement is reported as 0.5% of the depth. One of the important parameters for depth and position

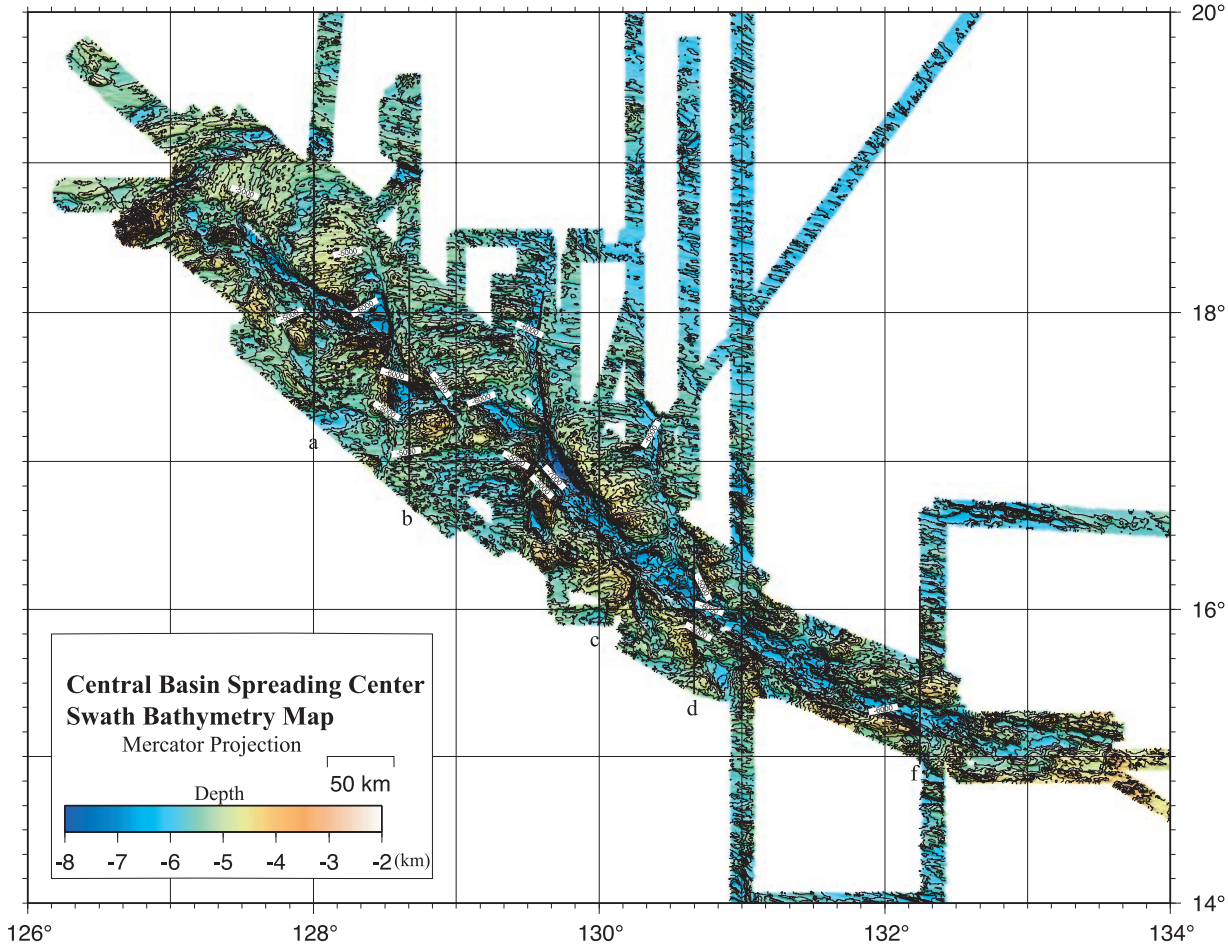

Figure 3. Shade relief bathymetry of the CBSC illuminated from north. Contour interval is 200 m. Across-axis profiles along the lines labeled as "a" to "f" are shown in Figure 9.

accuracy of the bathymetric survey is the sound velocity profile. SeaBeam 2112 system uses the velocity data not only for calculating the depth and position of each beam but also for the beam-forming process. The temperature of the surface layer is most important in this regard, and the system measures and uses surface temperature in real time. During our cruises, data from expendable bathythermograph (XBT) measurements were used to about 1830 m. We removed extreme depth variations from the outer edge of the swath. The chosen grid size is 150 m, and the swath is masked to approximately the original swath coverage, allowing interpolation of small gaps within 1 km. The shaded relief map, illuminated from the north with a 100-m contour interval, and the tectonic fabric extracted from the swath bathymetry are shown in Figures 3 and 4, respectively.

[13] For the Fourier transform analyses described below, a complete bathymetry grid without gaps was required. To achieve this, a 2-min bathymetry grid predicted from satellite-derived gravity anomaly [*Smith and Sandwell*, 1997] was merged with shipboard data to produce a smoothed data set with a reduced grid spacing of 1 min.

[14] The shipboard free-air gravity data from four cruises were merged with navigation and filtered along-track using a weighted averaging procedure to reduce short-period noise. Drift and the Eotvos corrections were made, and the free-air gravity anomaly was calculated using the standard gravity formula. The internal crossover errors of free-air anomalies in each cruise are within 3–4 mGal. A DC-shift of less than 15 mGal was applied to minimize the crossover errors among the four cruises. These corrected data from four cruises were combined and gridded in 1-min cells. Small data gaps within the survey are was interpolated using satellite gravity [*Sandwell and Smith*, 1997]. The 10-mGal contour map made from this grid is shown in Figure 5.

[15] In order to estimate the crustal thickness of the area we calculated the MBA [*Lin et al.*, 1990]. The gravity effects of the water-seafloor and the crust-mantle interfaces were forward modeled following the method described by *Parker* [1972] using the 1-min bathymetry grid. A density contrast of 1800 kg/m^3 was assumed at the seafloor and one of 500 kg/m^3 for the Moho. The Moho was assumed to lie everywhere 5 km below the seafloor. The calculated gravity effects of both interfaces were gridded and then subtracted from the gridded free-air gravity anomaly. The resulting MBAs are contoured at 10-mGal intervals in Figure 6. The MBA at midocean ridges primarily reflects crustal thickness variations [*Lin et al.*, 1990]. Other contributors to the MBA include the thermal effects of plate cooling with age and subcrustal density variations related to the pattern of mantle

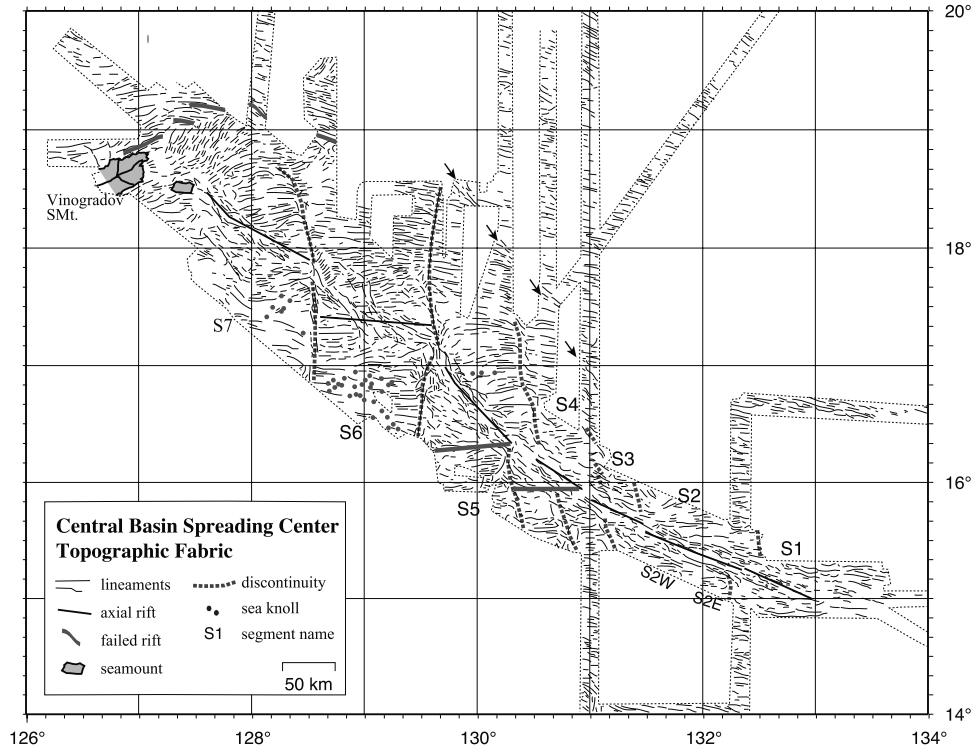

Figure 4. Seafloor fabric chart. Several important tectonic components, such as axial rifts, failed rifts, segment discontinuities, and sea knolls, are recognized. The segments are labeled as S1–S7.

upwelling, temperature variations, and the distribution of partial melt [*Lin and Phipps-Morgan*, 1992]. The CBSC is not an active ridge system; therefore, the contributions from the latter parameters can be neglected in this discussion.

[16] Shipboard total-field magnetic anomaly data (International Geomagnetic Reference Field (IGRF1995) removed) from four cruises were compiled. The crossover errors show unusually large values, sometimes larger than 100 nT. The large DC-shift between cruises is due to uncertainties in the time-varying coefficients that determine the IGRF; this is especially evident as the surveyed area is far from the magnetic observatories deciding the IGRF. We therefore recalculated the anomalies by using DGRF1995 and IGRF2000, obtaining a significant decrease in the shift between cruises. Another factor contributing to decreased accuracy is solar disturbance. The period of the survey cruises, during the later 1990s, corresponds to a period of increased solar activity: some magnetic storms and small-scale disturbances occurred during the survey. The closest available magnetic observatory is Langpang (Taiwan), 800 km NW of the study area, so an accurate diurnal correction could not be obtained. In consequence the derived gridded data set (1 min) still includes erroneous values, and the data quality is not high enough to stand detailed discussion or further processing. The 25-nT contour map shown in Figure 7 therefore serves primarily as an indicator of the rough pattern of seafloor magnetic characteristics.

4. Results

4.1. On-Axis and Off-Axis Morphology

[17] The compiled SeaBeam bathymetry data (Figure 3) are shown in the form of a contoured shaded-relief map. The large morphological variations along the CBSC reflect the complex tectonic history of this area. The morphology and segmentation characteristics have important implications for the nature of the spreading process of the CBSC because the morphotectonic variability between segments may be controlled by a combination of plate separation rates, asthenospheric flow patterns and temperatures, and magma supply. For most midocean ridges first-order discontinuities are defined by transform faults where strike-slip motion is concentrated in a narrow zone. Second-order discontinuities, at slow spreading ridges, are defined by nontransform discontinuities with small offsets (<30 km) and off-axis traces, while overlapping spreading centers are observed at fast-spreading ridges [*MacDonald et al.*, 1988, 1991; *Grindlay et al.*, 1991]. The segmentation pattern of the CBSC between the Kyushu-Palau Ridge and 126°30′E is characterized by one long-lived transform fault (129°34′E), five nontransform discontinuities, and one overlapping spreading center. The segments between these discontinuities have been numbered in sequence from east to west (Figure 4). In this section we point out four basic observations of the on-axis and off-axis morphology in the surveyed area. More detailed descriptions of each morphological feature are given in the Appendix.

1. The discontinuities and morphological features exhibit both ''slow-spreading'' features and ''fast-spreading'' characteristics, although the spreading rate is estimated as 36 mm/yr at the cessation of spreading, with no significant changes along the axis [*Hilde and Lee*, 1984]. The three eastern discontinuities are typical nontransform discontinuities with off-axis traces of nodal deeps; these exhibit ''slow-spreading'' characteristics. In contrast, the westernmost segment exhibits an overlapping spreading center

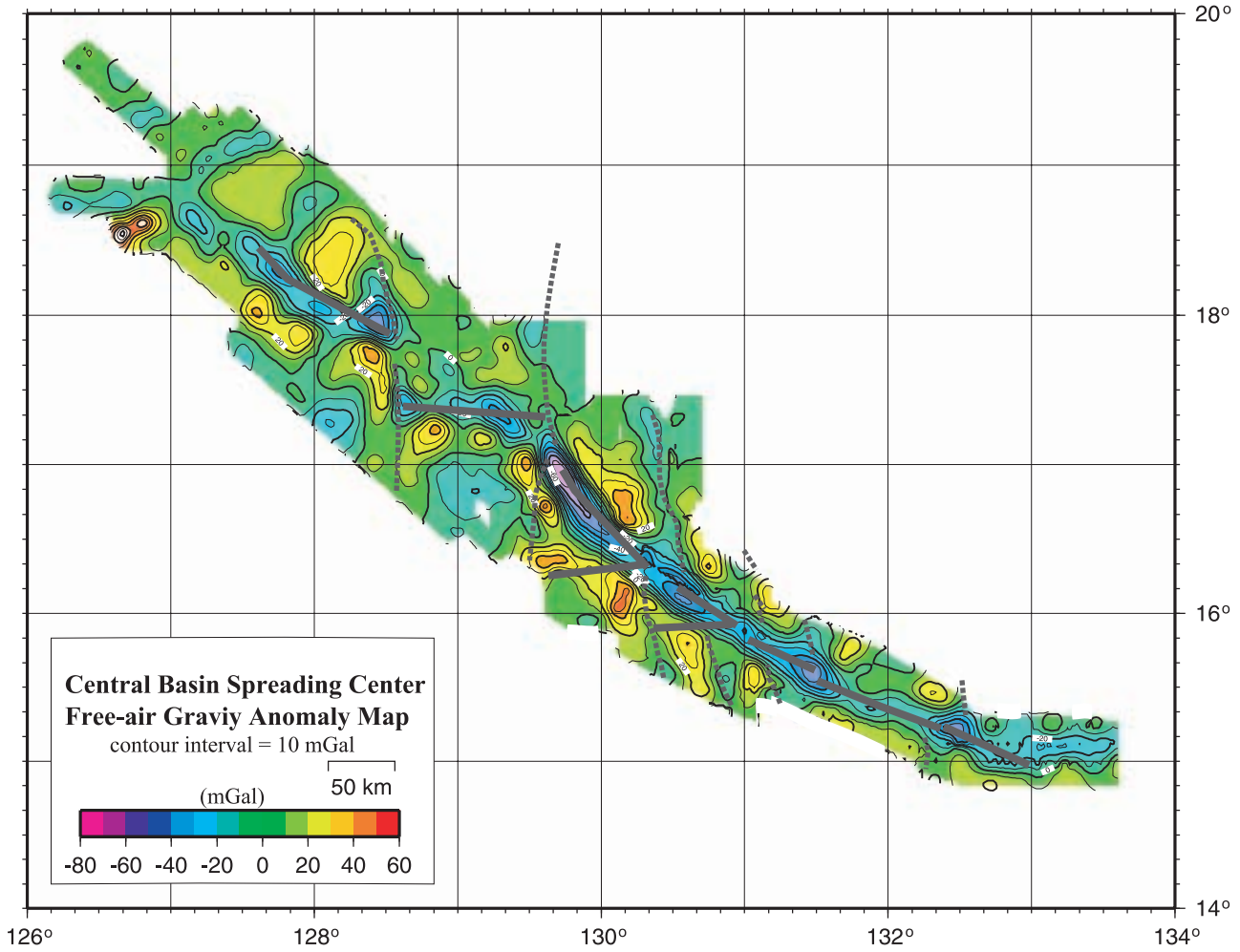

Figure 5. Free-air gravity anomalies contoured at 10-mGal intervals. Thick lines show the axial rifts identified with bathymetry.

geometry typical of fast spreading ridges (Figure 8). A major bathymetric feature in the area is a series of abandoned rifts near 16°N that show a left-stepping en echelon alignment and form a sinuous escarpment. The morphology and alignment of the abandoned rifts resembles the geometry of failed rifts in the "cyclic failure" rift propagation model [*Wilson*, 1990]. Across-axis bathymetry profiles (Figure 9a) show that the relief of the abyssal hills is smoother in the western segments S6 and S7, in contrast to the rough seafloor east of 131°30′E. The roughness indicator "MAD" (Median Absolute Deviation [*Small*, 1994]) also shows increasing roughness in the eastern CBSC (Figure 9b), although the MAD values are rather scattered. These results indicate a marked difference in magma supply along the CBSC. Two large seamounts located at segment S7 (Figure 8) also suggest that a higher magma supply existed in the western segment of the CBSC.

2. The seafloor more than 45 km from the CBSC shows relatively continuous NW-SE trending fabric, which supports the interpretation of NE-SW-directed spreading at intermediate rates in the early stages of the formation of the WPB [*Hilde and Lee*, 1984]. Between 129°45′ and 131°00′E some oblique (about 135°), narrow depressions that abut the NW-SE fabric are recognized on the swath bathymetry map (small arrows in Figure 4). These are interpreted as pseudofaults associated with eastward propagation of the ridge segment. On the other hand, north-south-directed spreading during the final formation stage of the WPB is confirmed by east-west-trending abyssal hills near the axis. A slight change of the off-axis fabric orientation from 095°, 080° and then 090° near the axial valley, suggests that spreading directions were highly variable or unstable during the latest stage of basin formation.

3. Deep rift valleys that are oblique to the 080°–095° trending off-axis abyssal hills are prominent along the entire CBSC. These rifts cut the spreading fabric, and they are interpreted to be the results of renewed tectonism after the cessation of north-south-directed spreading. Segment S6 is the best segment to understand the complicated history of the CBSC. The axial rift valley and abyssal hills trend east-west, and oblique lineaments and grabens trending NW-SE are overprinted on this older spreading fabric. The oblique rifts are observed over the entire CBSC, although their characteristics differ between segments. We consider that the oblique feature is a result of NE-SW extension that postdates the formation of the basin floor and was constrained by the

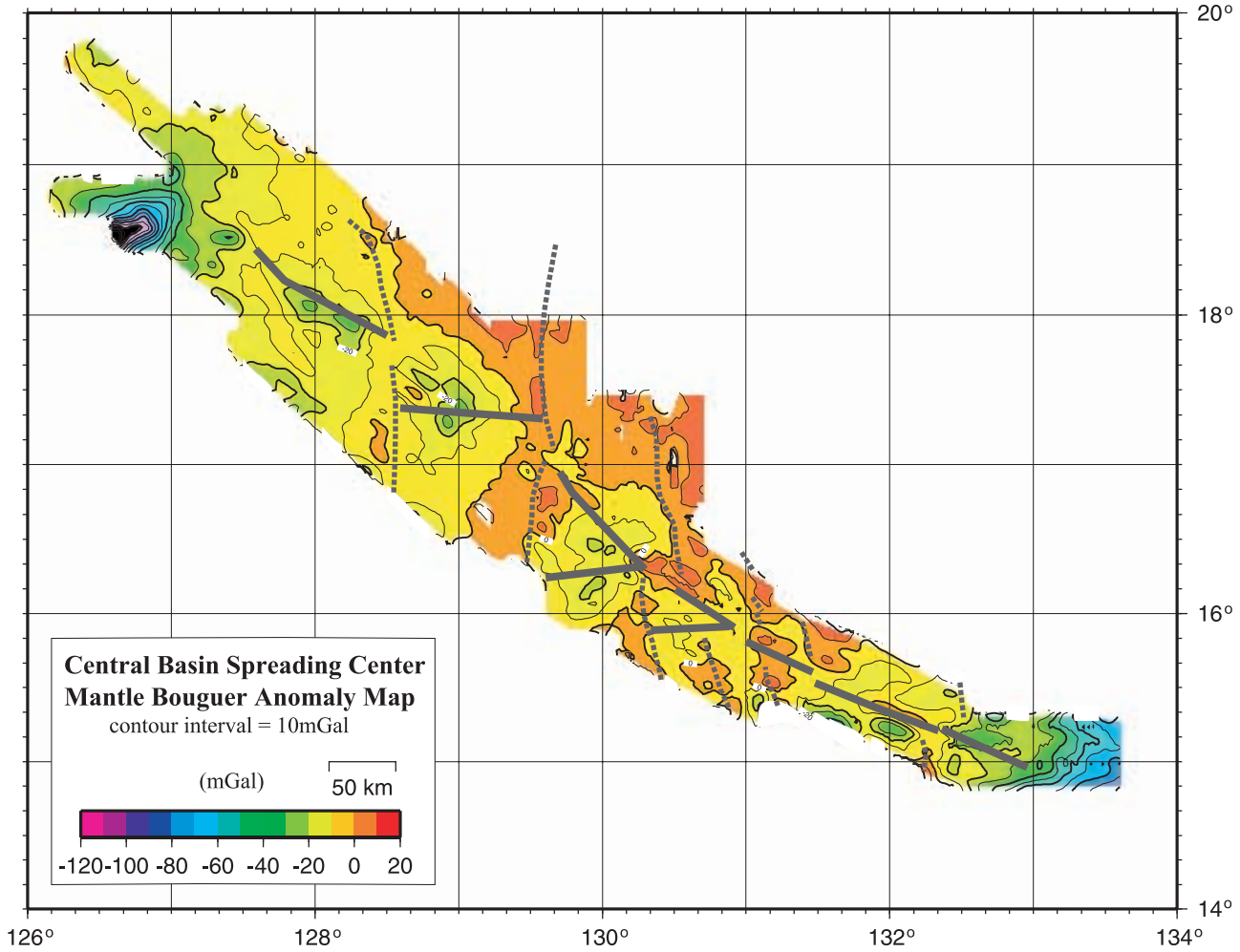

Figure 6. MBAs contoured at 10-mGal intervals. Thick lines show the axial rifts identified with bathymetry.

preexisting crustal architecture. The existence of the triangular nodal basins at 16°18′N in S5 and at 16°10′E in S4 support the idea that the older east-west spreading axes are located south of the oblique rift and that the rift developed by linking the old segment ends.

4. The offset of axial discontinuities across the rift axis is observed for all discontinuities east of the 129°34′E fracture zone. The break in the northern rift wall at the intersection with the off-axis trace of the discontinuity is located east of the corresponding break in the southern rift wall. This indicates the existence of a right-lateral sense of shear component in the latest stage of tectonism.

4.2. Gravity Anomaly

[18] Off-axis free-air anomalies away from large topographic features generally ranges from −10 to 10 mGal (Figure 5). Large positive anomalies are associated with the rift flank mountains (40 mGal) and with a large seamount (>80 mGal) at the westernmost end of the area. Negative anomalies are measured in deep oblique rifts and deep basins within the rift valley. Small negative anomalies are found over the off-axis traces of the eastern axial discontinuities and over the abandoned rifts at the northwestern end of the survey area. These free-air anomalies generally reflect topographic relief. Most of the smaller-scale features related to bathymetric relief in the free-air anomalies are removed in the MBA calculations (Figure 6). The large seamount at the western end of the survey area exhibits a −120 mGal MBA low reflecting thicker crust beneath the seamount. Large negative MBAs are also found in the eastern end of the area, indicating the existence of a thick root supporting the Kyushu-Palau Ridge. The large negative anomalies along the oblique deep rifts are nearly eliminated by the topographic correction.

[19] Figure 6 shows the segmentation and the along-axis variation of the subsurface structure in the CBSC. The 129°34′E fracture zones and eastern nontransform discontinuity traces are associated with higher positive MBA anomalies, probably reflecting thinned crust formed at segment ends resulting from three-dimensional upwelling, similar to slow spreading ridges. A circular MBA low of −20 mGal is observed at the midpoint of Segment S6. The eastern segments are also associated with MBA lows; however, the centers of the negative anomalies are not at the midpoints of the deep rift valleys. These MBA lows of −20 mGal are centered a few tens of kilometers south of the deep rift valleys, where the topographic fabric trends approximately 090°. This indicates that, in terms of the

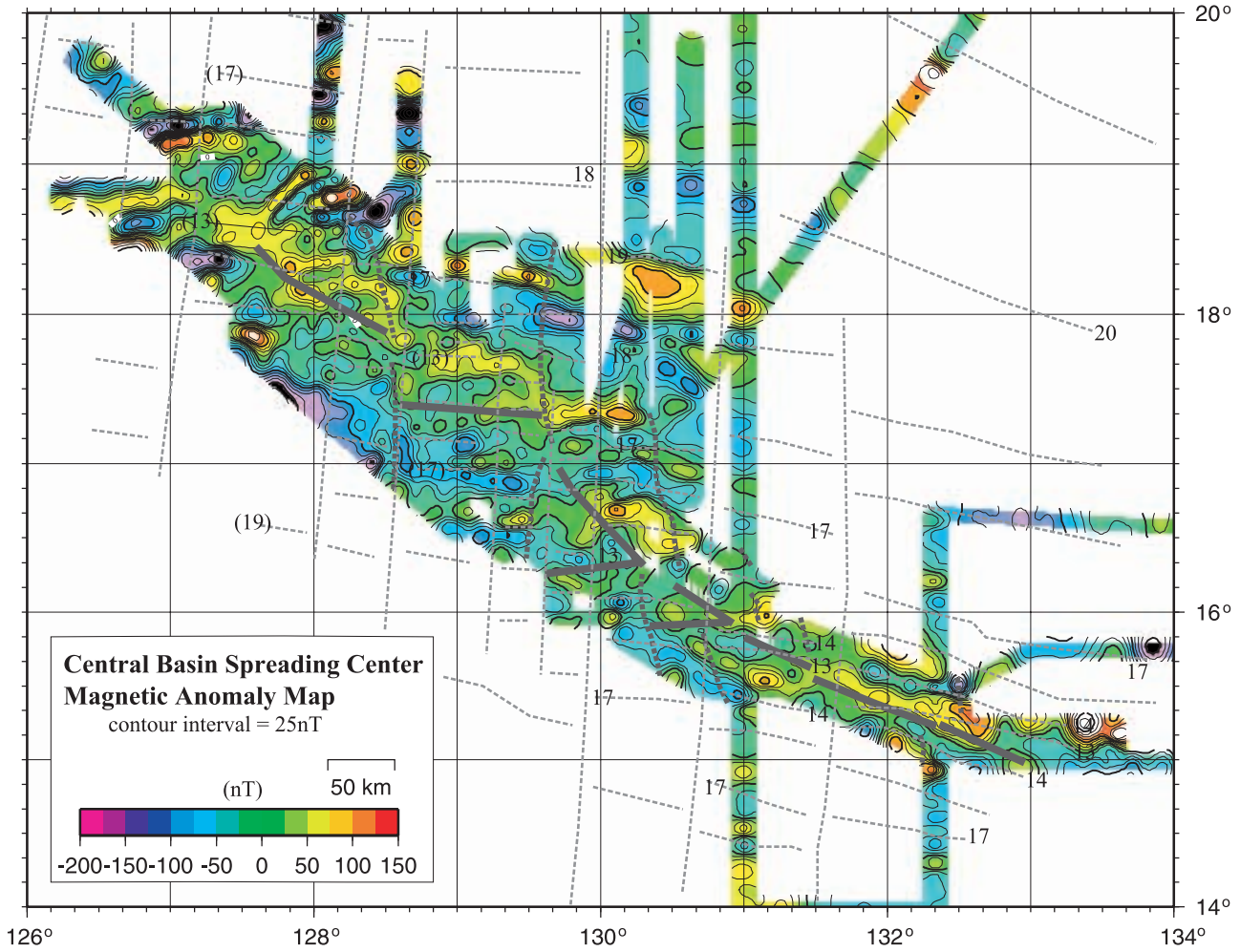

Figure 7. Total field magnetic anomalies contoured at 25-nT intervals. Thick lines show the axial rifts identified with bathymetry. Thin lines and numbers are magnetic anomaly lineations identified by *Hilde and Lee* [1984].

density structure, the spreading segment centers are located to the south of the deepest rift valleys. The quasi-triangular depression on the swath bathymetry map is found west of the MBA minimum, and we interpret this depression as an extinct nodal basin at the original ridge-transform intersection. Along S7, the westward propagating rift containing the overlapping spreading center (OSC), the −20 mGal MBA contour line defines an ellipse elongated along the rift valley. The off-axis MBA values are also lower in the western part. This may reflect thicker crust beneath the western segments, suggesting vigorous magmatism in this area. In contrast, small positive anomalies are recognized above the oblique rifts, especially in S2E, S4, and the western part of S5, suggesting amagmatic extension in these rifts.

[20] Circular MBA lows at segment midpoints, called "bull's-eyes," are typically observed in active slow spreading centers [e.g., *Kuo and Forsyth*, 1988; *Lin et al.*, 1990; *Detrick et al.*, 1995; *Thibaud et al.*, 1998]. These are commonly interpreted in terms of variations in crustal thickness, crustal or mantle density, and the thermal effects of upwelling at the ridge axis. The crust is interpreted to be thicker beneath the segment midpoints and thinner beneath the segment ends. The residual MBA pattern, after removing thermal effects, exhibit a band of low MBA from the segment center toward the off-axis areas instead of "bull's-eyes," indicating the contribution of melt-rich upwelling mantle diapir beneath the ridge axis [*Lin et al.*, 1990]. Although the CBSC is an extinct spreading center where the thermal effects should be negligible, "bull's-eyes" patterns are observed. Similar gravity anomalies have been recognized in other extinct spreading centers (Labrador Sea, CBSC, Coral Sea, and Magellan Trough) by *Jonas et al.* [1991]. They indicated that a frozen-in low-density structure is confined to within about 10 km of either side of the extinct axis, which is consistent with the presence of a gabbroic root beneath the axis. On the other hand, *Olser and Louden* [1992, 1995] showed that the combination of thin crust and serpentinized upper mantle due to the reduction of melt supply during the death of the spreading system could explain both the gravity anomaly and seismic structure beneath the Labrador Sea. Either case is plausible for the CBSC, and distinguishing between them is not possible with the currently available data. Regardless, circular MBA lows along the CBSC correspond to

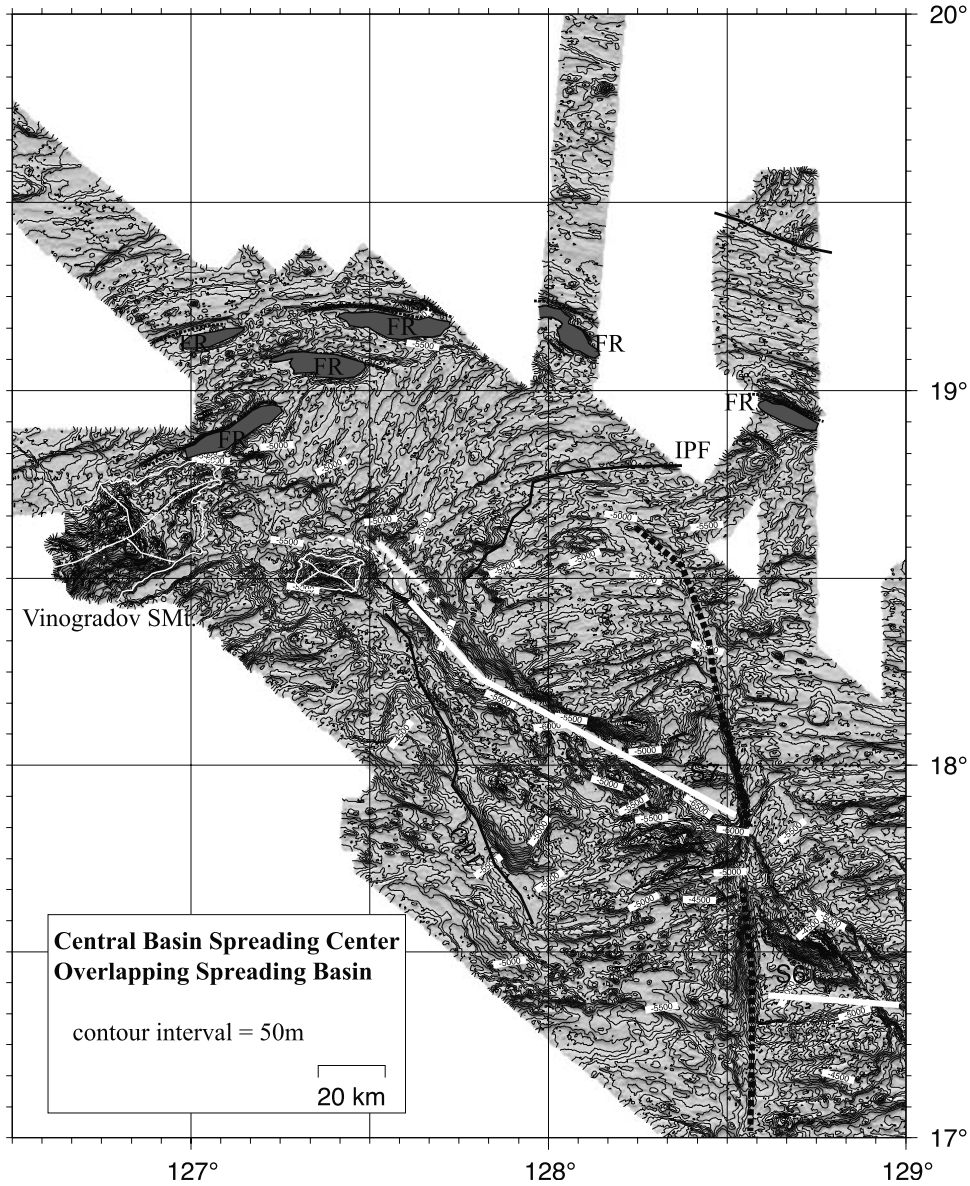

Figure 8. Detailed shaded relief bathymetry with 100-m contours in the western part of the CBSC. Tectonic components, such as failed rifts and oblique lineaments, show the overlapping spreading. FR, failed rift; IPF, inner pseudo-fault; OPF, outer pseudo-fault.

locations of spreading segment centers at the time that the system died, and the off-axis extent of low MBAs in the western segments indicates thicker crust in the western region.

4.3. Magnetic Anomalies

[21] The limited off-axis survey, the ridge parallel survey lines, and relatively low quality of the original data make it difficult to identify the anomaly lineations and to discuss the magnetization of the ridge axis. Therefore we only point out three important pieces of information derived from Figure 7.

[22] First, the east-west-trending magnetic lineations are offset by fracture zones and discontinuities, indicating north-south-directed spreading and segmentation of the ridge axis in the later phases of spreading. A set of oblique lineations is observed in the area north of segment S7, supporting the existence of the OSCs. The previous identification of magnetic anomalies [*Hilde and Lee*, 1984] shown in dotted lines with numbers in Figure 7 is generally consistent with our data east of S6; however, reexamination may be required to understand the detailed segmentation patterns of the western part of the CBSC.

[23] Second, the anomaly pattern shows rough symmetry about the axis at S6 (indicated in Figure 7), and the offset between S6 and S5 is approximately 90 km. The axis of S5, estimated from the magnetic anomaly pattern, is coincident with the location of the relict east-west-trending rift and with the location of the MBA minimum. No clear anomaly pattern is associated with the oblique rifts in S5. This indicates that the oblique rifts were formed by postspreading amagmatic tectonism.

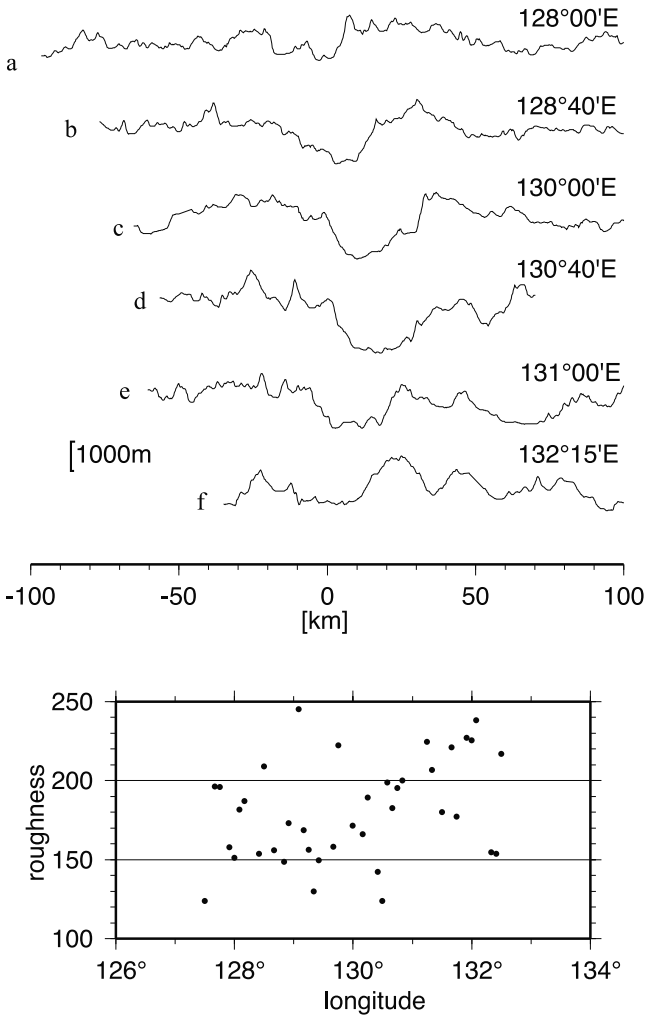

Figure 9. (top) Across-axis bathymetry profiles. The locations of six profiles are shown in Figure 3. (bottom) Bathymetry roughness versus longitude. Roughness is defined as the MAD of the residual profile, which is obtained by removing the first five modes from the original profile.

[24] Third, the highest positive anomalies are parallel to the oblique rifts and are observed north of segments S1 and S2. These may be related to the latest volcanic activities.

4.4. Along-Axis Variation

[25] Along-axis variation in bottom topography and MBAs are shown in Figure 10 to demonstrate both segment-scale variation and long-wavelength trends along the CBSC. The thin lines indicate the profile along the deepest point of the rift valley, including the oblique rifts in the eastern segments. The thick gray lines indicate the 090°-trending extinct spreading center identified from the swath bathymetry and the location of MBA lows. Both lines are shown in plan view in Figure 4. In general each segment center is associated with a local topographic maximum. Segment S2 exhibits a local minimum at the segment midpoint that is interpreted as a higher-order discontinuity between S2E and S2W. The western segments S6 and S7 exhibit rather flat bottom profiles within the segment, while the profiles of the eastern segments are nearly sinusoidal. Segment midpoints are well correlated with local minima of MBAs. The ridge segments defined by the MBA lows reflect the underlying crust and mantle structure well and correspond to the volcanic segmentation. The along-axis half-segment MBA gradient (as defined by *Lin and Phipps-Morgan* [1992]) for S7 is 0.26 mGal/km, which is similar to gradients observed at the fast-spreading East Pacific Rise (EPR) [e.g., *Wang and Cochran*, 1993]. The MBA low at the segment midpoint is largest at S6, where the MBA relief exceeds 25 mGal, and the gradient is 0.58 mGal/km, which is similar to values reported from the Mid-Atlantic Ridge [e.g., *Lin and Phipps-Morgan*, 1992; *Detrick et al.*, 1995]. The eastern segments, S1 and S2, have relatively high MBA gradients, similar to those described on slow-spreading ridges. The characteristics of segments change at the 129°34′E transform fault. The average MBA is low in the western segments S6 and S7, and the average depth is a little shallower. The segment length is also longer compared with eastern segments. These results may reflect the higher melt supply in the western CBSC.

5. Discussion

5.1. The Origin of "Fast-Spreading" Features in the Western CBSC

[26] The westernmost part of the survey area exhibits unique characteristics as follows: (1) smoother and slightly shallower bathymetry, (2) overlapping spreading center geometry, and (3) low MBA in off-axis areas. The en echelon, short, deep troughs and sets of oblique lineaments resemble features observed near microplates or OSCs typical of fast spreading ridges. Abyssal hills created by the westward-propagating ridge change orientation from almost east-west to 080° near the 128°36′E discontinuity, similar to the change in orientation of abyssal hills spread from segments S5 and S6. The 110°-trending rift valley extends to 127°00′E and cuts the abyssal hill fabric at an oblique angle, so the valley was formed after dueling propagation. The MBA low is centered near the midpoint of S7; however, the −20 mGal contour is elongated, not circular. The low MBA area is not focused along the extinct spreading center but encompasses the off-axis seafloor west of 128°35′E. This indicates thick crust beneath the western part of the CBSC, probably reflecting higher rates of melt production.

[27] The western CBSC exhibits "fast-spreading" features, although the full spreading rate was 36 mm/yr in the north-south-directed spreading stage of the West Philippine Basin [*Hilde and Lee*, 1984]. In contrast, the eastern CBSC shows typical slow-spreading features such as rough abyssal hills and nontransform discontinuities (NTDs). Although the Euler pole and angular velocity of spreading along the CBSC have not been established, the limited length of the surveyed spreading center and the trend of the abyssal hills support the idea that differences in spreading rate between the eastern and western survey areas were small. These data and observations support the interpretation that, although spreading rate is clearly an important parameter controlling ridge morphology and segmentation [*MacDonald*, 1982;

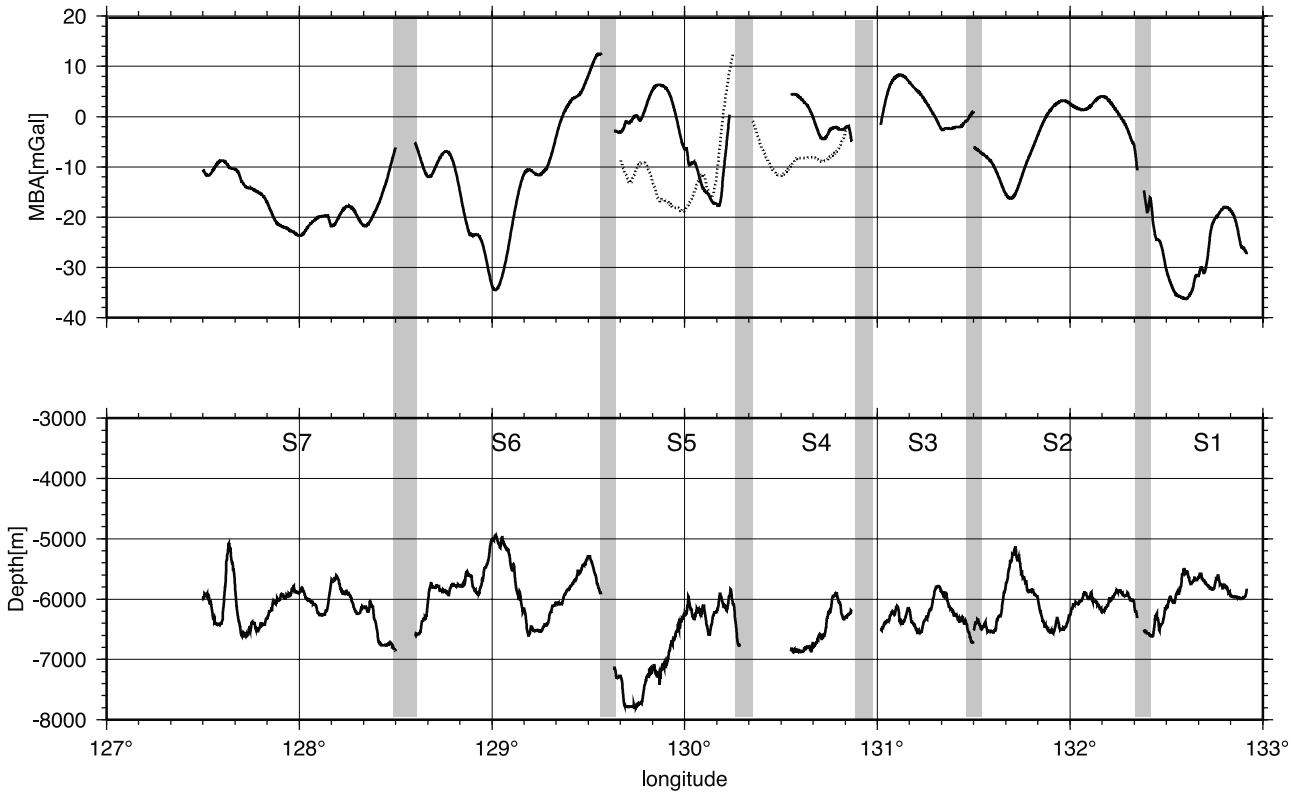

Figure 10. (top) Along-axis variations in MBA and (bottom) depth along the CBSC. Thick lines are profiles along the latest rift system, including oblique deep rifts in segments S4 and S5. Gray lines illustrate the values along the rifts of north-south spreading. The locations of axial rifts are shown in Figure 4.

Lin and Phipps-Morgan, 1992], there should be other control factors deciding the spreading style.

[28] The effect of thermal structure on ridge morphology and segmentation is clearly seen along the Southeast Indian Ridge (SEIR), where the ridge spreads at a narrow range of intermediate rates but exhibits the full range of slow-spreading to fast-spreading features [*Cochran et al.*, 1997; *Sempere et al.*, 1997; *Small et al.*, 1999]. The western SEIR is characterized by a long-wavelength increase in axial depths, OSCs, and large negative MBAs, whereas deeper axial valleys, nontransform discontinuities, and higher MBAs are observed toward the Australian-Antarctic Discordance (AAD). This large variation in the style of crustal accretion can be attributed to a gradient in mantle temperature between regions influenced by the Amsterdam and Kerguelen hot spots and the AAD [*Sempere et al.*, 1997]. Similar along-axis variations are also reported for ridges near hot spots, e.g. the Azores hot spots [*Detrick et al.*, 1995]. In general, ridge-hot spot interaction causes robust magmatism, which forms thicker crust and resultant shallow seafloor.

[29] *Niu et al.* [2001] emphasize the importance of mantle compositional control on the extent of mantle melting, crust production, gravity anomaly, ridge morphology, and segmentation. They analyze the observed difference between two segments of the Mid-Atlantic Ridge (MAR) between the Oceanographer and Hayes transforms, where the mantle potential temperature is the same and the plate spreading rate is the same. They demonstrate that morphological differences are ultimately controlled by variations in fertile mantle source composition, as reflected in lava chemistry. Samples from the magmatically robust segment are more enriched in incompatible elements, total alkalis, and H_2O contents relative to samples from the magma-starved segment. Their results indicate that the heterogeneity of fertile mantle source composition is important as are mantle temperature and plate spreading rate variations.

[30] The ''fast-spreading'' morphology and large MBA lows (indicating thicker crust) in the western CBSC are interpreted to be the result of higher rates of melt production. Although the CBSC is not presently active and the velocity structure obtained by seismic tomography does not directly reflect the thermal structure during the period of basin formation, the shear wave velocity of the upper mantle beneath the CBSC exhibits relatively low velocities in the western part of the basin [*Nakamura and Shibutani*, 1998]. This may reflect remnant high mantle temperatures during basin formation.

[31] On the other hand, variations in basalt geochemistry along the CBSC may point to heterogeneity of the upper mantle source, requiring no variation in potential temperature. As described in section 4.2, large blocky seamounts are located near and within the rift west of 127°30′E. The westernmost seamount, centered at 126°45′E, 18°35′N, has relief greater than 4000 m and is delineated by 070°-trending troughs (Figure 3). Dredge sampling operations

were carried out by a Russian vessel at this seamount [*Shcheka et al.*, 1995], named the Vinogradov Seamount. The sampled basalts are classified in the leucocratic potassium-sodium group, characterized by low abundances of mafic elements (Cr, Ni) and anomalously high contents of lithophyle elements (P, Ba, Sr, Zr, and Rb). These characteristics match the composition of Ocean Island Basalt (OIB). Based on the satellite altimetry map, the Vinogradov Seamount is located at the northern end of a seamount chain extending from the Benham Rise. The Benham Rise is a relatively small but significant oceanic plateau at the westernmost edge of the WPB (Figure 2). It was probably formed by volcanism near the CBSC and was moved toward its present position by seafloor spreading [*Hilde and Lee*, 1984]. DSDP Site 292 was drilled on the southern Benham Rise, where basement consisting of olivine tholeiite was recovered [*Karig*, 1975]. The basalt chemistry bears out the OIB-like character of the Benham Rise by its much higher TiO_2 and other high field strength element (HFSE) composition [*Hickey-Vargas*, 1998]. These signatures could reflect heterogeneous upper mantle, which could be explained by the contamination of the upper mantle by mantle plumes. The geophysical and geochemical observations support the idea that the ''fast-spreading'' characteristics and thicker crust along the western CBSC were influenced by hotter upper mantle and/or by heterogeneous mantle source. And the heterogeneity of upper mantle may be due to local contamination by a small-scale mantle plume, which formed the plateaus in the western WPB. Although no plumes are found in the WPB at present, tectonic reconstruction of the Philippine Sea Plate [*Hall et al.*, 1994] places it north of Australia at 50 Ma, above the plume-rich Indian Ocean asthenospheric domain [*Hickey-Vargas*, 1998]. The large geophysical variations along the CBSC and the ''fast-spreading'' to ''slow-spreading'' characteristics may reflect variations in the underlying thermal/chemical structure of the asthenosphere.

5.2. Development of the CBSC

[32] Tectonic spreading fabric typically parallels spreading center segments, and fracture zones are generally orthogonal to spreading segments. Adjacent to the CBSC, however, we observe multiple orientations of lineaments, reflecting a more complicated history. Although the full bathymetric coverage is somewhat limited, coverage along the remnant spreading axis and up to 45 km away from the CBSC shows three stages of seafloor spreading as follows: (1) NE-SW spreading (Figure 11a), (2) north-south spreading (Figures 11b and 11c) and (3) NE-SE rifting (Figure 11d). The first and second stages are generally similar to the scenario proposed by *Hilde and Lee* [1984]; however, we have documented a more detailed picture of development of the CBSC.

[33] The seafloor generated during the first NE-SW-directed spreading stage can only be seen along some north-south transit lines in our map. The orientation of the lineaments varies from 120° in the north to 105° near the axis. The abyssal hills are relatively continuous, and their relief is relatively low, which may indicate stable intermediate rate spreading (88 mm/yr, *Hilde and Lee* [1984]). The fracture zone at 129°34′E has existed since this period, based on the satellite altimetry map, although no fracture zone is recognized north of 18°30′N in Figure 3. The Benham Rise and the Urdaneta Plateau were formed near the ridge at that time, which was influenced by higher mantle temperatures beneath the western CBSC. The spreading fabric trends 045° at the northern end of line 128°40′E (small arrow in Figure 8). These resemble the set of lineaments seen in the overlapping spreading basin near the axis, so these may be related to an older dueling propagation. This indicates that the western part of the basin also exhibited ''fast-spreading'' features in the earlier stages of basin genesis. In contrast, east of the 129°34′E fracture zone, 135°-trending troughs oblique to the spreading fabric are seen on four survey lines (small arrows in Figure 4). These troughs appear to be long pseudo-faults related to eastward segment propagation, indicating that the segment east of this pseudo-fault decreased in length as the basin developed (Figure 11a). The sense of propagation shows that the temporal evolution of segmentation is affected by the thermal regime in the underlying mantle and asthenosphere, which is reported at Mid-Atlantic Ridge near the Azores hot spot [*Phipps Morgan and Parmentier*, 1985; *Thibaud et al.*, 1998].

[34] The second-order discontinuities between segments S3, S4, S5, and S6 can be traced about 35 km from the axial rift both on the swath map (Figure 4) and the satellite altimetry data. The spreading direction changes from NE-SW to almost north-south at that point. This change in pole location and plate motion vectors was accommodated by breakup of the spreading axes into multiple smaller segments offset by discontinuities (Figure 11b), preserving the overall NW-SE-trending thermal structure. The relief of the east-west abyssal hills is higher than that of the NW-SE fabric formed earlier, which may indicate that the spreading rate decreased at the time of the change of extension direction. A similar change of spreading style, i.e., rotation of spreading axis, higher segmentation, and spreading rate decrease, is also observed in the final stages of other back arc basins in the Philippine Sea [*Okino et al.*, 1999].

[35] During the north-south-directed spreading stage, a slight change of spreading direction is recognized from the geometry of abyssal hills and fracture zones (Figure 11c). It is most clearly seen in segment S6, where the trend of abyssal hills rotates progressively from 095°, 080° to 090° near the rift valley. The fracture zone at 129°35′E also changed orientation to 173°, corresponding to the orientation of the abyssal hills and resulting in the formation of an arcuate escarpment. The same change can be observed in the off-axis seafloor of the eastern segments, although the fabric is disturbed by later deformation. This indicates that the spreading regime was unstable near the end of basin formation. The location of the MBA centers and the magnetic lineations suggest that the youngest east-west ridge segments are located south of the present-day deep rift and that the small deep depressions at the end of the relict ridges are remnant nodal basins. In the western part of the CBSC, the dueling propagators formed an overlapping spreading basin between them.

[36] The main part of the WPB was formed in the above-mentioned first and second stages. The third stage is essentially amagmatic and takes the form of NE-SW-directed rifting. This created fault scarps, grabens, and extremely

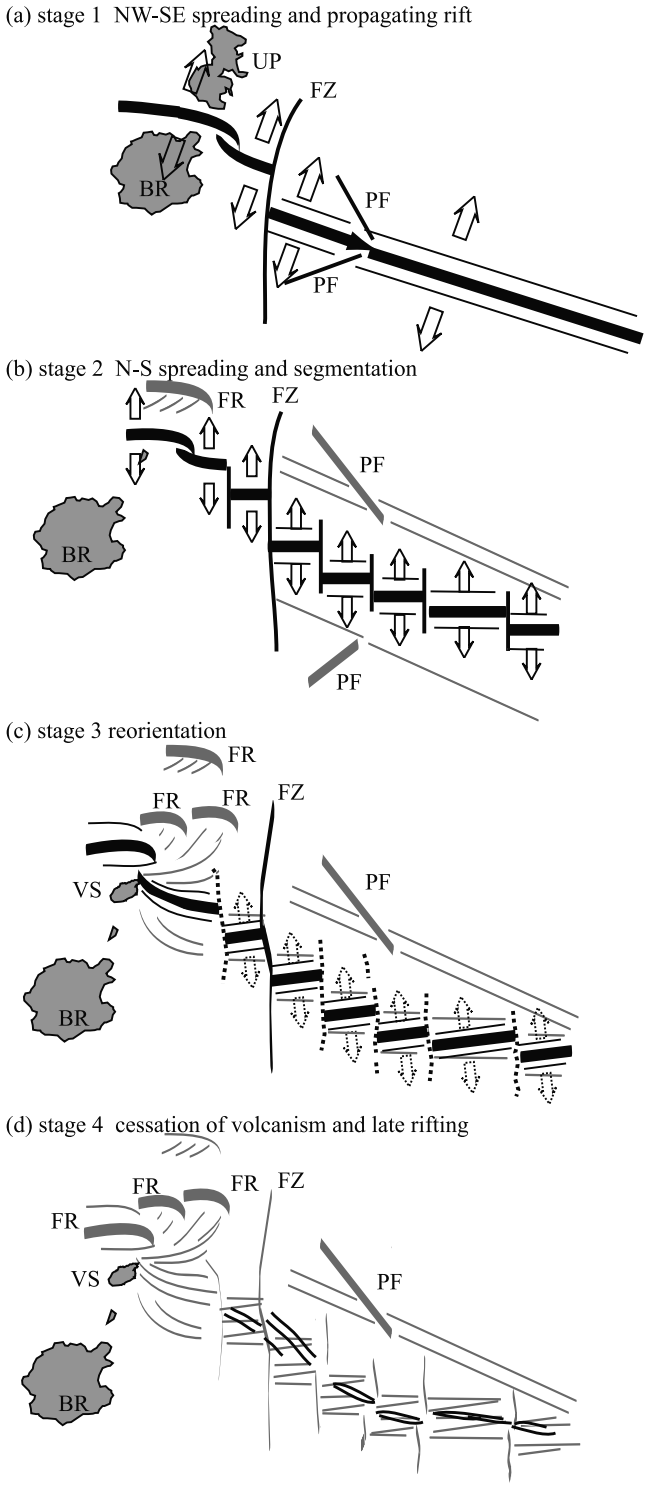

Figure 11. Schematic figures of the evolution of the CBSC. FR, failed rift; FZ, fracture zone; PF, pseudo faults; BR, Benham Rise; VS, Vinogradov Seamount; UP, Urdaneta Plateau. (a) NW-SE-spreading phase. The Benham Rise is formed near the CBSC in the western basin. Eastern segments propagate toward east. (b) North-south spreading phase. The ridge axis are segmented. The western part of the CBSC is characterized by cyclic dueling propagation. (c) Spreading direction is unstable in the last phase of the basin formation. (d) Cessation of volcanism and postspreading deformation forming oblique rifts.

deep valleys cutting the preexisting fabric formed by north-south-directed seafloor spreading. It is also responsible for the offset of nontransform discontinuities in a right-lateral sense. Deformation is concentrated in the areas surrounded by adjacent segment ends (Figure 11d). This may indicate that the deformable zone was constrained by the thermal regime (and hence the mechanical properties of the lithosphere) inherited from the earlier stages of seafloor spreading. The amount of deformation is smaller in the western segments of the CBSC; the deep rift valleys develop in the segments east of the 129°34′E fracture zone. We suggest that this difference was caused by the difference of subsurface structure between the eastern and western CBSC. This stage is tectonic dominant and generally amagmatic; however, some evidence of volcanism occurs on the seafloor. In segments S1 and S2, elongated minor ridges located within the rift valley may be the youngest axial volcanic zones. Figure 7 shows that segments S2 and S3 have positive magnetic anomalies along the central rift, although the other part of the CBSC is occupied by negative anomalies. This suggests that a late magmatic phase occurred in the eastern segment.

[37] We did not infer an absolute timescale for the evolutionary history of the CBSC. It is hard to identify magnetic lineations based only on our results because of the along-axis survey line direction. The most widely supported evolutionary model of the WPB [*Hilde and Lee*, 1984] proposes a NE-SW-directed opening at 88 mm/yr between 56 and 45 Ma (Anomaly 22) followed by a north-south-directed opening at 36 mm/yr that ceased at 35 Ma (Anomaly 13). However, recent age dating of rock samples from the CBSC indicates younger ages than previously reported. Two basalt samples from the oblique rift at S5 [*Fujioka et al.*, 1999] have ages of 28.10 ± 0.16 ($^{40}Ar/^{39}Ar$), 26.1 ± 0.9 (K/Ar), and 14.88 ± 0.16 Ma ($^{40}Ar/^{39}Ar$). Some K/Ar dates are also reported from the CBSC: 27.4 [*Okino et al.*, 1999] and 16.2 Ma [Ohara, pers. commun.] at S1. Though the K/Ar data may include large errors due to degassing, there is a peak around 27 Ma, which is younger than the previous model [*Hilde and Lee*, 1984]. We examined two scenarios: (1) slow (35 mm/yr) north-south spreading ceased at 35 Ma, then minor amounts of volcanism occurred along the remnant axis around 27 and 15 Ma; and (2) slow north-south spreading ceased at 27 Ma, and the minor activity occurred at 15 Ma because a large percentage of the age data indicate that volcanism occurred at this time. We prefer the former one because the second scenario required a completely new identification of magnetic anomalies, and we do not have any evidence denying the *Hilde and Lee* [1984] identification. The age of 27 Ma for the volcanism in the CBSC is almost the same age as that of the eastern Parece Vela Basin opening [*Okino et al.*, 1998]. The cessation of spreading and/or the final extensional stage are probably related to the opening of the back arc basin along the Kyushu-Palau Ridge. Compiled heat flow measurement in the Philippine Sea Plate [*Yamano and Kinoshita*, 1995] show relatively higher values along the CBSC, suggesting that either active tectonism or minor volcanism has occurred since the basin ceased spreading. Magmatic activity after basin formation at a remnant spreading axis is also reported at the Kinan Seamount Chain in the Shikoku Basin [*Sakamoto and Kim*, 1999; *Ishii et al.*, 2000] and at

the Scarborough Seamount Chain in the South China Sea [*Wang et al.*, 1985].

5.3. Implication for the Reconstruction of the West Philippine Basin

[38] This paper focuses on the tectonics of the extinct spreading center rather than the genesis of the whole basin. However, these new data have some implications for the reconstruction of the WPB.

[39] First, the western part of the basin is closely associated with ocean plateau formation. The Benham Rise and some small seamounts were formed near the CBSC, where the basalt chemistry shows OIB-like character. The western CBSC exhibits prominent OSC geometry. This apparent "fast-spreading" morphology is attributed to the higher magma supply related to elevated mantle temperatures or a heterogeneous mantle source. The northwestern part of the basin was mapped by the Japan Hydrographic Department [*Okino et al.*, 1999], and there is evidence for failed rifts and oblique sets of lineaments [*Yoshida et al.*, 2000]. These data suggest that the western part of the basin has had a higher magma supply for a long time. The segment propagation in the WPB was perhaps influenced by its rate.

[40] Second, the age of cessation of WPB formation is still equivocal. There are several viable ages given for the halt of volcanism in the WPB, 35 [magnetic anomaly, *Hilde and Lee*, 1984], 27, and 15 Ma [$^{40}Ar/^{39}Ar$ dating, *Fujioka et al.*, 1999]. These various ages raise several possibilities for the rifting in the basin. If the 35 Ma age is correct, then the later volcanism is related to reactivation after a hiatus. Another possibility is that the central part of the basin is younger than has been previously considered. The dating results and the rifts on the topographic high at the intersection with the Kyushu-Palau Ridge provide the evidence for activity of the CBSC even in the stage of back arc opening of the eastern Philippine Sea. The ages reported along the CBSC have not yet been compiled and are scattered in a relatively large range, partly due to inaccurate K/Ar dating. However, the age data have two reliable peaks at 26–27 and 15 Ma, so the volcanism continued after basin formation. Oblique rifts were also formed after basin formation, although the timing is not known. These postspreading activities may reflect a general reorganization of plate motions in the region.

[41] Third, the off-axis morphology shows a more complicated history of the basin than that proposed by *Hilde and Lee* [1984]. Recently a large escarpment (the Oki-Daito Escarpment, Figure 2) was reported in the northern part of the WPB, north of which the spreading fabric indicates north-south-directed opening [*Ohara et al.*, 1998; *Okino et al.*, 1999]. Pseudo-faults indicating propagating ridges are also recognized in our data set. Although there has been no systematic survey in the southern Philippine Sea until now, a clear linear structure crossing the basin can be mapped on the satellite-derived gravity map (Figure 1), which may be a candidate for the counter part of the Oki-Daito Escarpment. Older side-scan data [*Andrews*, 1980] and single-swath data by R/V *l'Atalante* [*Deschamps*, 1999] show large variations of the spreading fabric on the basin floor. In order to reconstruct the detailed history of the basin, recompilation of the magnetic anomaly, recent age dating, and the fragments of known tectonic fabric data should be combined.

6. Conclusions

[42] We have studied the morphological and geophysical characteristics of the extinct CBSC between 126°00′ and 133°30′E. Our study supports the following conclusions:

1. Along the CBSC the ridge segments and discontinuities exhibit a morphological range from typical slow-spreading features in the eastern segments to fast spreading features in the westernmost segment. The spreading rate is almost the same in this geographically limited area; therefore, this variety is related to the rate of magma supply relative to spreading rate.

2. The western part of the CBSC is characterized by overlapping spreading centers, extensive MBA lows, and smoother off-axis bathymetry. These fast-spreading features are in striking contrast with the eastern CBSC, showing a typical slow-spreading character. We consider that the observed differences are caused by variations in crustal thickness along the CBSC resulting from higher melt supply in the western CBSC.

3. Relics of cyclic rift failure caused by dueling propagation that are found in the northwestern part of the basin indicate that higher melt supply may have affected the western WPB throughout basin formation. The proposed increased melt supply may reflect higher mantle temperatures suggested by previous seismic topography results [*Nakamura and Shibutani*, 1998] or reflect heterogeneity in upper mantle geochemical composition due to mantle plume contamination, suggested by OIB-like signatures of basalt samples [*Hickey-Vargas*, 1998].

4. Based on the orientation of abyssal hills, the latest stage of the WPB opening is characterized by north-south-directed spreading from a highly segmented ridge. The prominent deep rift and lineaments obliquely cut these abyssal hills, indicating that an amagmatic rifting stage occurred after the main basin formed. The oblique features are observed only between ridge-transform intersection zones, suggesting that inherited mechanical and/or thermal characteristics may have controlled the expression of postspreading deformation. Circular MBA lows are centered at the east-west-trending extinct ridge axis, not at the oblique deep rift. This indicates that the anomalous density structure beneath the spreading center is preserved after the cessation of spreading.

5. New age data from the CBSC axis range from 27 to 15 Ma. These dates indicate that reactivation or deformation along the CBSC continued long after the basin formed and may be related to the opening of the Parece Vela Basin.

[43] Our results indicate that higher magma supply, perhaps related to a small mantle plume, is a key factor controlling the morphological and geophysical variations along the CBSC. This elevated magma supply affected not only the spreading style but also the evolutionary history of the basin.

Appendix A: Detailed Description of Morphological Features

A1. On-Axis and Off-Axis Morphology

[44] We define seven segments and intervening discontinuities mainly based on swath bathymetry data along the CBSC (Figures 3 and 4); however, we used supplementary

Table 1. Segments and Discontinuities of the CBSC Between 126°00′ and 133°30′E

Name	Length 1[a], km	Length 2[a], km	Maximum Rift Width, km	Average Depth, m	Rift Height, m	Trend, deg	Neo Volcanic Zone (NVZ)
S1	61		19	5900	1500	115°	yes
S2	100	123	19	6500	1100–1500	112°	yes
S2E	49					114°	yes
S2W	51					110°	?
S3	57	44	25	6400	1400, 109°	No	
S4	40	46	23	6800	1300, 123°	No	
S5	109	83	26	7700	1600–2800	138°	no
S6	107	107	20	6000	900–1500	092°	no
S7	90		20	6200	1300	116°	no
S8	(series of failed rifts in our survey area)						

				Off-Axis Trace	
Name	Location	Type	Offset	Our Map	Satellite
S1–S2	132°21′E NTD		not clear	ambiguous	
S2E–S2W	131°55′E		no	very short	
S2–S3	131°30′E NTD		yes	yes	
S3–S4	130°52′E NTD		yes	yes	
S4–S5	130°17.5′E	NTD		yes	yes
S5–S6	129°34′E ETF & FZ[b]		yes	yes	
S6–S7	129°30′E short TF[c]		yes	yes	
S7–S8		OSC		yes	

[a]Length is measured along the current deepest rift, and Length 2 is the distance between discontinuities at both ends.
[b]FZ, fracture zone.
[c]TF, transform fault.

satellite-derived gravity anomaly data [*Sandwell and Smith*, 1997] for detecting the off-axis traces of discontinuities. The locations of discontinuities, segment length, rift valley relief and rift wall elevation, and other parameters are summarized in Table 1. All segments are right-laterally offset by the discontinuities and preserve the general NW-SE trend inherited from the earlier NE-SW-directed spreading stage. Segment length, defined here as the distance between neighboring discontinuities, ranges from 44 to 123 km. The longest segment, S2, can be divided into two third-order segments, S2W and S2E. These have approximately the same length as the second-order segments, but the offset between them has no off-axis trace.

[45] The off-axis seafloor is primarily characterized by linear abyssal hills indicating continuous seafloor spreading from the CBSC. The general trend of the abyssal hills gradually varies from 110° to 080°, except for the area west of 128°30′E, where oblique lineaments formed by the OSC are found. The orientation of the off-axis fabric changes from 095° far from the axis, to 080° and 090° near the axial rift. This change can be most clearly seen in S6 but is a common feature along other segments. The 129°34′E fracture zone changes orientation by 10° (from 003° to 353°) north of the rift valley. The location of this change is approximately coincident with the disappearance of the nontransform discontinuity traces, suggesting that ridge segmentation and reorganization compensated for the change of spreading direction.

[46] The deep rifts oblique to the off-axis fabrics are observed over the entire CBSC, but detailed characteristics differ between segments. In Segment S1, where the east-west-trending rift is wider than in the other segments, two 115°-trending, en echelon rifts are developed within the east-west-trending rift. Small ridges about 200 m high located in the oblique rifts may reflect weak volcanism during rifting. The oblique rift trends about 110° in S2 and S3, where the rift shoulder mountains are characterized by east-west lineaments but are interrupted by the oblique rifts at the axial zone. Two 200-m-high ridges are located symmetrically within the oblique rift at S2W, which suggests that they are the remnants of a neovolcanic zone split by extensional tectonics. The very deep and highly oblique rifts deform the east-west-spreading fabric in S4 and S5. The axis of symmetry in the older east-west-spreading fabric is located south of the oblique rift.

A2. The Western CBSC Overlapping Spreading Center

[47] Just west of the 128°36′E discontinuity the seafloor fabric is similar to the fabric observed in segment S6, where the orientation of abyssal hills varies from east-west to 080° near the axis. The 140°E-trending central rift becomes indistinct between 127° and 127°30′E. A major bathymetric feature in the area is a series of abandoned rifts near 16°N that show a left-stepping en echelon alignment, indicating successive rift failures. The seafloor fabric between these failed rifts and the 140°E-trending rift valley exhibits a variation from almost east-west to a 030° trend. The area also has a shallow average depth when compared with other off-axis areas. The abandoned rifts seem to have been created by successive rift failures with a short repeat cycle. The western (northern) ridge segment, which is not numbered in this paper, was abandoned while the eastern segment (S7) propagated westward.

[48] The length and width of the overlap region are ~100 km, so that the length to width ratio is close to 1:1. The OSC is typical of those seen at fast spreading centers, e.g., the East Pacific Rise, the Pacific-Cocos, and the Pacific-Antarctic plate boundaries. Large-scale dueling propagation forms trapped microplates similar to the Easter microplate

[*Handschumacher et al.*, 1981; *Hey et al.*, 1985; *Naar and Hey*, 1991] or the Juan Fernandez microplate [*Francheteau et al.*, 1987; *Larson et al.*, 1992; *Martinez et al.*, 1997]. Small-scale OSCs are observed at second-order discontinuities along fast-spreading centers.

[49] At 126°45′E, 18°30′N, a large seamount higher than 3000 m is located south of the diminishing rift valley. The surrounding area is characterized by 075°-trending lineaments, and the seamount itself is bounded by faults with the same orientation. This may reflect some structural control of volcanic construction. The horizontal scale and volume of the mountain are estimated to be 90 × 30 km and 3000 km^3, respectively, although our survey does not cover the entire mountain. To the east a smaller but similarly structurally controlled seamount whose length and height are 15 km and 2000 m is located at the center of the rift valley. This seamount shows a marked contrast to the small axial volcanic ridges observed in S1 and S2. These observations suggest that a higher magma supply existed in the western segment of the CBSC.

[50] Small seamounts with relief <600 m are closely spaced on the southern flanks of segments S6 and S7 (indicated by a small dot in Figure 4). The typical size of these seamounts is a 5–7 km diameter. Similar size seamounts are also located in the off-axis areas of the eastern segments, but they are more widely distributed. The seamount cluster coincides with a MBA low, suggesting thicker crust and presumably more abundant magmatism than in eastern areas.

[51] **Acknowledgments.** We thank the captain and crew of R/V *Kairei* for their efficient work during the STEPS cruises. We also thank T. Hilde, E. Honza, T. Yamazaki, S. Lallemand, A. Deschamps, and all the onboard scientists for data acquisition and useful discussion. Constructive reviews of the manuscript by K. Tamaki and D. Curewitz are greatly appreciated. Y. Ohara, O. Ishizuka, and H. Sato gave us valuable information and comments from the viewpoint of petrology. Thanks also to F. Martinez, an anonymous reviewer, and the Associate Editor for their helpful comments.

References

Andrews, J. E., Morphologic evidence for reorientation of sea-floor spreading in the West Philippine Basin, *Geology*, *8*, 140–143, 1980.

Ben-Avraham, Z., C. Bowin, and J. Segawa, An extinct spreading center in the Philippine Sea, *Nature*, *240*, 453–455, 1972.

Caress, D. W., and D. N. Chayes, Improved processing of Hydrosweep DS multibeam data on the R/V Maurice Ewing, *Mar. Geophys. Res.*, *18*, 631–650, 1996.

Cochran, J. R., and J.-C. Sempere, The Southeast Indian Ridge between 88°E and 118°E: Gravity anomalies and crustal accretion at intermediate spreading rates, *J. Geophys. Res.*, *102*, 15,463–15,487, 1997.

DeMets, C., R. G. Gordon, D. F. Argus, and S. Stein, Current plate motions, *Geophys. J. Int.*, *101*, 425–478, 1990.

Deschamps, A., S. Lallemand, and S. Dominguez, The last spreading episode of the West Philippine Basin revisited, *Geophys. Res. Lett.*, *26*, 2073–2076, 1999.

Detrick, R. S., H. D. Needman, and V. Renard, Gravity anomalies and crustal thickness variations along the Mid-Atlantic Ridge between 33°N and 40°N, *J. Geophys. Res.*, *100*, 3767–3787, 1995.

Francheteau, J., A. Yelles-Chaouche, and H. Carig, The Juan Fernandez microplate north of the Pacific-Nazca-Antarctic plate junction at 35°S, *Earth Planet. Sci. Lett.*, *86*, 253–268, 1987.

Fujioka, K., T. Kanamatsu, A. Sasaki, Y. Ohara, I. Sakamoto, S. Haraguchi, and T. Ishii, Morphology and geology of extinct spreading center in the Philippine Sea Plate—Results of the Yokosuka Y96-11 cruise, *JAMSTEC J. Deep Sea Res.*, *13*, 155–194, 1997.

Fujioka, K., et al., Morphology of Mariana Trench and Central Basin Fault—Preliminary results of KR9801 cruise, *JAMSTEC J. Deep Sea Res.*, *14*, 163–192, 1998.

Fujioka, K., K. Okino, T. Kanamatsu, Y. Ohara, O. Ishizuka, S. Haraguchi, and T. Ishii, An enigmatic extinct spreading center in the West Philippine backarc basin unveiled, *Geology*, *27*, 1135–1138, 1999.

Fujioka, K., et al., Parece Vela Rift and Central Basin Fault revisited—STEPS-IV (Structure, Tectonics and Evolution of the Philippine Sea)—Cruise summary report, *InterRidge News*, *9*(1), 18–22, 2000.

Grindlay, N. R., P. J. Fox, and K. C. MacDonald, Second-order ridge axis discontinuities in the south Atlantic: Morphology, structure, and evolution, *Mar. Geophys. Res.*, *13*, 21–50, 1991.

Hall, R., J. R. Ali, C. D. Anderson, and S. J. Baker, Origin and motion history of the Philippine Sea Plate, *Tectonophysics*, *251*, 229–250, 1995.

Handschumacher, D. W., R. H. Pilger, J. A. Foreman, and J. R. Campbell, Structure and evolution of the Easter plate, *Mem. Geol. Soc. Am.*, *154*, 63–76, 1981.

Haston, R. B., and M. Fuller, Paleomagnetic data from the Philippine Sea plate and their tectonic significance, *J. Geophys. Res.*, *96*(B4), 6073–6098, 1991.

Hess, H. H., Major structural features of the western north Pacific, and interpretation of H.O. 5989 bathymetric chart, Korea to New Guinea, *Geol. Soc. Am. Bull.*, *59*, 417–446, 1948.

Hey, R. N., D. F. Naar, M. C. Kleinrock, W. J. Phipps-Morgan, E. Morales, and J.-G. Schilling, Microplate tectonics along a superfast seafloor spreading system near Easter Island, *Nature*, *317*, 320–325, 1985.

Hickey-Vargas, R., Origin of the Indian Ocean-type isotopic signature in basalts from Philippine Sea plate spreading centers: An assessment of local versus large-scale processes, *J. Geophys. Res.*, *103*(B9), 20,963–20,979, 1998.

Hilde, T. W. C., and C.-S. Lee, Origin and evolution of the West Philippine Basin: A new interpretation, *Tectonophysics*, *102*, 85–104, 1984.

Ishii, T., H. Sato, S. Machida, S. Haraguch, A. Usui, O. Ishizuka, H. Taniguchi, and K. Yagi, Geological and petrological studies of the Kinan and Izu-Ogasawara-back arc-echelon Seamount Chains, *Bull. Geol. Surv. Jpn.*, *51*(12), 615–630, 2000.

Jonas, J., S. Hall, and J. Casey, Gravity anomalies over extinct spreading centers: A test of gravity models of active centers, *J. Geophys. Res.*, *96*, 11,759–11,777, 1991.

Karig, D. E., Basin genesis in the Philippine Sea, in *Initial Reports of the Deep Sea Drilling Project*, vol. 31, edited by D. E. Karig et al., pp. 857–879, U.S. Govt. Print. Off., Washington, D. C., 1975.

Klein, G. V., and K. Kobayashi, Geological summary of the North Philippine Sea, based on Deep Sea Drilling Project Leg 58 results, in *Initial Reports of the Deep Sea Drilling Project*, vol. 58, edited by G. Glein et al., pp. 951–961, U.S. Govt. Print. Off., Washington, D. C., 1981.

Kroenke, L., et al., *Initial Reports of the Deep Sea Drilling Project*, vol. 59, U.S. Govt. Print. Off., Washington, D. C., 1980.

Kuo, B. Y., and D. W. Forsyth, Gravity anomalies of the ridge transform system in the South Atlantic between 31 and 34.5°S: Upwelling centers and variations in crustal thickness, *Mar. Geophys. Res.*, *10*, 205–232, 1988.

Larson, R. L., R. C. Searle, M. C. Kleinrock, H. Schouten, R. T. Bird, D. F. Naar, R. I. Rusby, E. E. Hooft, and H. Lasthiotakis, Roller-bearing tectonic evolution of the Juan Fernandez microplate, *Nature*, *356*, 571–576, 1992.

Lewis, S. D., and D. E. Hayes, The structure and evolution of the Central Basin Fault, West Philippine Basin, in *The Tectonic and Geologic Evolution of Southeast Asian Islands*, *Geophys. Monogr. Ser.*, vol. 23, edited by D. E. Hayes, pp. 77–88, AGU, Washington, D. C., 1980.

Lin, J., and J. Phipps-Morgan, The spreading rate dependence of three-dimensional mid-ocean ridge gravity structure, *Geophys. Res. Lett.*, *19*, 13–16, 1992.

Lin, J., G. M. Purdy, H. Schouten, J.-C. Sempere, and C. Zervas, Evidence from gravity data for focused magmatic accretion along the Mid-Atlantic Ridge, *Nature*, *344*, 627–632, 1990.

Louden, K. E., Magnetic anomalies in the West Philippine Basin, in *The Geophysics of the Pacific Ocean Basin and Its Margins*, *Geophys. Monogr. Ser.*, vol. 19, edited by G. H. Sutton, M. H. Manghnani, and R. Moberly, pp. 253–267, AGU, Washington, D. C., 1976.

MacDonald, K. C., P. J. Fox, L. J. Perrm, M. F. Eisen, R. M. Haymon, S. P. Miller, S. M. Carbotte, M.-H. Cormier, and A. N. Shor, A new view of the mid-ocean ridge from the behaviour of ridge-axis discontinuities, *Nature*, *335*, 217–225, 1988.

MacDonald, K. C., D. S. Scheirer, and S. M. Carbotte, Mid-ocean ridges: Discontinuities, segments and giant cracks, *Science*, *253*, 986–994, 1991.

Martinez, F., R. N. Hey, and P. D. Johnson, The east ridge system 28.5–32°S East Pacific rise: Implications for overlapping spreading center development, *Earth Planet. Sci. Lett.*, *151*, 13–31, 1997.

Mizuno, A., Y. Okuda, S. Nagumo, H. Kagami, and N. Nasu, Subsidence of the Daito Ridge and associated basins, north Philippine Sea, in *Geologi-*

cal and Geophysical Investigations of Continental Margins, vol. 29, edited by J. S. Watkins, L. Montadert, and P. W. Dickerson, pp. 239–243, Am. Assoc. of Pet. Geol., Tulsa, Okla., 1978.

Mrozowski, C. L., S. D. Lewis, and D. Hayes, Complexities in the tectonic evolution of the West Philippine Basin, *Tectonophysics*, *82*, 1–24, 1982.

Naar, D. F., and R. N. Hey, Tectonic evolution of the Easter microplate, *J. Geophys. Res.*, *96*, 7961–7993, 1991.

Nakamura, Y., and T. Shibutani, Three-dimensional shear wave velocity structure in the upper mantle beneath the Philippine Sea region, *Earth Planets. Space*, *50*, 939–952, 1998.

Niu, Y., D. Bideau, R. Hekinian, and R. Batiza, Mantle compositional control on the extent of mantle melting, crust production, gravity anomaly, ridge morphology and ridge segmentation: A case study at the Mid-Atlantic Ridge 33–35°N, *Earth Planet. Sci. Lett.*, *186*, 383–399, 2001.

Nur, A., and Z. Ben-Avraham, Oceanic plateaus, the fragmentation of continents, and mountain building, *J. Geophys. Res.*, *87*, 3644–3661, 1982.

Ohara, Y., S. Kasuga, K. Okino, and Y. Kato, Survey maps: Philippine Sea structure, *EOS Trans AGU*, *78*, 555, 1997.

Okino, K., Y. Ohara, S. Kasuga, and Y. Kato, The Philippine Sea: New survey results reveal the structure and the history of the marginal basins, *Geophys. Res. Lett.*, *26*, 2287–2290, 1999.

Osler, J. C., and K. E. Louden, Crustal structure of an extinct rift axis in the Labrador Sea: Preliminary results from a seismic refraction survey, *Earth Planet. Sci. Lett.*, *108*, 243–258, 1992.

Osler, J. C., and K. E. Louden, Extinct spreading center in the Labrador sea: Crustal structure from a two-dimensional seismic refraction velocity model, *J. Geophys. Res.*, *100*, 2261–2278, 1995.

Ozima, M., I. Kaneoka, and H. Ujiie, ^{40}Ar-^{39}Ar ages of rocks and the development mode of the Philippine Sea, *Nature*, *267*, 816–818, 1977.

Park, C.-H., K. Tamaki, and K. Kobayashi, Age-depth correlation of the Philippine Sea back-arc basins and other marginal basins in the world, *Tectonophysics*, *181*, 351–371, 1990.

Parker, R. L., The rapid calculation of potential anomalies, *Geophys. J. R. Astron. Soc.*, *31*, 447–455, 1972.

Parmentier, E. M., and J. Phipps Morgan, Spreading-rate dependence of three-dimensional structure in oceanic spreading centers, *Nature*, *348*, 325–328, 1990.

Phipps Morgan, J., and E. M. Parmentier, Causes and rate-limiting mechanisms of ridge propagation: A fractures mechanism model, *J. Geophys. Res.*, *90*, 8603–8613, 1985.

Sakamoto, I., and Y.-U. Kim, Petrographical characteristics of volcanic rocks sampled from Kosyu Seamount, northern part of Shikoku Basin, *Bull.Tokai Univ.*, *48*, 145–159 (in Japanese with English abstract), 1999.

Sandwell, D., and W. H. F. Smith, Marine gravity anomaly from Geosat and ERS 1 satellite altimetry, *J. Geophys. Res.*, *102*, 10,039–10,054, 1997.

Sclater, J. G., Heat flow and elevation of the marginal basins of the western Pacific, *J. Geophys. Res.*, *77*, 5705–5719, 1972.

Scott, R., and L. Kroenke, Evolution of back arc spreading and arc volcanism in the Philippine Sea: Interpretation of Leg59 DSDP results, in *The Tectonic and Geologic Evolution of Southeast Asian Islands*, *Geophys. Monogr. Ser.*, vol. 23, edited by D. E. Hayes, pp. 283–291, AGU, Washington, D. C., 1980.

Sempere, J.-C., and J. R. Cochran, The Southeast Indian Ridge between 88°E and 118°E: Variation in crustal accretion at constant spreading rate, *J. Geophys. Res.*, *102*, 15,489–15,505, 1997.

Seno, T., and S. Maruyama, Paleogeographic reconstruction and origin of the Philippine Sea, *Tectonophysics*, *102*, 53–84, 1984.

Shcheka, S. A., S. V. Vysotskiy, V. T. S'edin, I. A. Tararin, Igneous rocks of the main geological structures of the Philippine Sea floor, in *Geology and Geophysics of the Philippine Sea*, edited by H. Tokuyama et al., pp. 251–278, Terra Sci., Tokyo, 1995.

Shih, T. C., Marine magnetic anomalies from the western Philippine Sea: Implications for the evolution of marginal basins, in *The Tectonic and Geologic Evolution of Southeast Asia Seas and Islands*, *Geophys. Monogr. Ser.*, vol. 23, edited by D. E. Hayes, pp. 49–75, AGU, Washington, D. C., 1980.

Small, C., A global analysis of mid-ocean ridge axial topography, *Geophys. J. Int.*, *116*, 64–84, 1994.

Small, C., J. R. Cochran, J.-C. Sempere, and D. Ghristie, The structure and segmentation of the Southeast Indian Ridge, *Mar. Geol.*, *161*, 1–12, 1999.

Smith, W. H. F., and D. T. Sandwell, Global seafloor topography from satellite altimetry and ship depth soundings, *Science*, *277*, 1956–1962, 1997.

Thibaud, R., P. Gente, and M. Maia, A systematic analysis of the Mid-Atlantic Ridge morphology and gravity between 15°N and 40°N: Constraints of the thermal structure, *J. Geophys. Res.*, *103*, 24,223–24,243, 1998.

Tokuyama, H., H. Kagami, and N. Nasu, Marine geology and subcrustal structure of the Shikoku Basin and the Daito Ridges region in the northern Philippine Sea, *Bull. Ocean Res. Inst.*, *22*, 1–169, 1986.

Uyeda, S., and Z. Ben-Avraham, Origin and development of the Philippine Sea, *Nature*, *240*, 176–178, 1972.

Wang, X., and J. R. Cochran, Gravity anomalies, isostasy and mantle flow at the East Pacific Rise crest, *J. Geophys. Res.*, *98*, 19,505–19,531, 1993.

Wang, X., M. Wu, D. Liang, and A. Yin, Some geochemical characteristics of basalts in the South China Sea, *Geochemistry*, *4*, 380–390, 1985.

Wessel, P., and W. H. F. Smith, New version of the Generic Mapping Tools released, *EOS Trans. AGU*, *76*, 329, 1998.

Wilson, D. S., Kinematics of overlapping rift propagation with cyclic rift failure, *Earth Planet. Sci. Lett.*, *96*, 384–392, 1990.

Yamano, M., and M. Kinoshita, Heat flow in the Philippine Sea, in *Geology and Geophysics of the Philippine Sea*, edited by H. Tokuyama et al., pp. 59–75, Terra Sci., Tokyo, 1995.

Yamazaki, T., K. Okino, Y. Hasegawa, H. Saitake, and M. Ito, Geophysical mapping of Mariana Trough and West Philippine Basin: A preliminary report of Kairei KR9812 cruise, *JAMSTEC J. Deep Sea Res.*, *15*(II), 63–72, 1999.

Yoshida, T., Y. Kato, Y. Ohara, and S. Kasuga, Various structures for activities of hotspots in the area south of the Shatsky Rise, in *Abstracts of 2001 Japan Earth and Planetary Science Joint Meeting*, A5-P006, Tokyo, 2000.

K. Fujioka, Japan Marine Science and Technology Center, Yokosuka, Japan.

K. Okino, Ocean Research Institute, University of Tokyo, 1-15-1 Minamidai, Nakano, Tokyo 164-8639, Japan. (okino@ori.u-tokyo.ac.jp)